

APPLICATION OF LAYER-BY-LAYER ASSEMBLY
FOR CONTROLLED DRUG RELEASE
FROM POLYGLYCOLIDE NANOPARTICLES

By

MENG WANG

Bachelor of Engineering in Pharmaceutical Engineering

College of Chemical Engineering and Technology

Tianjin University

Tianjin, P. R. China

2009

Submitted to the Faculty of the
Graduate College of the
Oklahoma State University
in partial fulfillment of
the requirements for
the Degree of
MASTER OF SCIENCE
December, 2012

APPLICATION OF LAYER-BY-LAYER ASSEMBLY
FOR CONTROLLED DRUG RELEASE
FROM POLYGLYCOLIDE NANOPARTICLES

Thesis Approved:

Dr. Heather Fahlenkamp

Thesis Adviser

Dr. Russ R. Rhinehart

Dr. Sundar V. Madhally

Dr. Sheryl A. Tucker

Dean of the Graduate College

TABLE OF CONTENTS

Chapter	Page
I. INTRODUCTION.....	1
1.1 Eye Anatomy, Diseases and Complications	2
1.2 Current Treatment Strategies for Eye Diseases	3
1.3 Controlled Drug Delivery Systems.....	5
1.4 Development of a Novel Ophthalmic Drug Delivery Device.....	6
II. LITERATURE REVIEW.....	8
2.1 Anatomy of the Eye	8
2.2 Controlled ocular drug delivery	12
2.2.1 Ophthalmic Hydrogels.....	12
2.2.2 Nanoparticles	14
2.2.3 Dendrimers.....	17
2.2.4 Drug-Loaded Contact Lenses	17
2.2.5 Implants.....	18
2.3 Layer-by-Layer Assembly for Drug Delivery	20
2.4 Selection of Model Drug.....	22
2.4.1 Core Material	22
2.4.2 Shell Material – Type I Collagen and Chitosan.....	24
2.5 Selection of Model Drug.....	26
III. REAGENTS, EQUIPMENT AND METHODOLOGY.....	28
3.1 Chemical Reagents.....	28
3.2 Equipment.....	29
3.3 Synthesis of Lidocaine-Loaded Polyglycolide Nanoparticles	29
3.4 Layer-by-Layer Entrapment.....	31
3.5 Size Distribution	32
3.6 Morphology.....	33
3.7 Zeta Potential	33
3.8 Fourier Transform Infrared Spectroscopy	35
3.9 Drug Loading.....	35
3.10 <i>In Vitro</i> Drug Release Profile	36
3.11 Statistical Methods.....	37
IV. RESULTS AND DISCUSSION.....	38
4.1 Size Distribution	38
4.2 Morphology.....	41
4.3 FTIR.....	43
4.4 Zeta Potential	43

Chapter	Page
4.5 Drug Loading	44
4.6 <i>In Vitro</i> Drug Release Profile	47
V. CONCLUSION AND FUTURE OUTLOOK	50
5.1 Conclusion	50
5.2 Future Outlook	51
REFERENCES	53

LIST OF TABLES

Table	Page
1. Chemical structures of some ophthalmic drugs	27
2. Average diameters for four nanoparticle samples	38
2. Drug loading contents for four nanoparticle samples	47

LIST OF FIGURES

Figure	Page
1. The anatomy of the eye.....	2
2. Details of novel ophthalmic drug delivery device.....	7
3. Physiological barriers of the eye.....	11
4. Schematic presentation of intravitreal route of drug delivery to posterior chamber of the eye.....	19
5. Layer-by-Layer assembly of polyelectrolytes on particles.....	21
6. Chemical structure of polyglycolide.....	23
7. The relationship between drug release and the four-stage degradation process...24	
8. Diagram showing a double-layer structure on a negative charged particle surface	35
9. Hydrodynamic size distribution.....	39
10. SEM images.....	42
11. FTIR spectra.....	43
12. Charge variation of alternative deposition.....	44
13. UV spectrum.....	45
14. Standard curve for lidocaine from concentration of 0.01 to 0.05 mg/ml.....	46
15. Drug release test in PBS, 37.4 °C.....	49

CHAPTER I

INTRODUCTION

The main objective of this work is to develop a better drug delivery system with more controllable release, better bioavailability, and convenient routes of use for topical administration of small hydrophobic ophthalmic drugs.

As revealed by the American Academy of Ophthalmology, millions of Americans suffer from eye diseases, most of which target at the posterior segment of the eye. [1] Some drugs have been developed to treat such eye diseases; however, it can be a challenge to deliver the drug to the posterior segment of the eye. Several barriers with effective defense mechanisms must be breached in order to deliver drug to the posterior segment of the eye. A drug delivery system to overcome these barriers was recently proposed and studied by a former graduate student of our research group. The proposed design included a thin, collagen membrane embedded with drug-loaded nanoparticles. Although this system was proved to deliver drug over an extended period, there was a sudden burst of 20 wt. % drug loading observed for the first 24 hours. The goal of the present project is to improve the previous system with less initial burst and extended drug

release. We propose to entrap the drug-loaded nanoparticles with mucoadhesive polyelectrolytes. The mucoadhesive coating materials will help with prolonging the residence time of the system as well as controlling the drug release rate. Furthermore, these coated nanoparticles can be easily administrated like eye drops without any side effects.

1.1 Eye Anatomy, Diseases and Complications

The eye is one of the most complicated organs in human body with many parts working for sense of sight. The eye is composed of the following two segments: (1) the anterior segment, which includes the cornea, iris, pupil, and lens, and (2) the posterior segment, which includes the vitreous body and retina. The main parts of the eye are shown in Fig. 1, and typically, the retina is the target for drug delivery for many eye diseases, since this is the only tissue of the eye that contains major blood vessels.

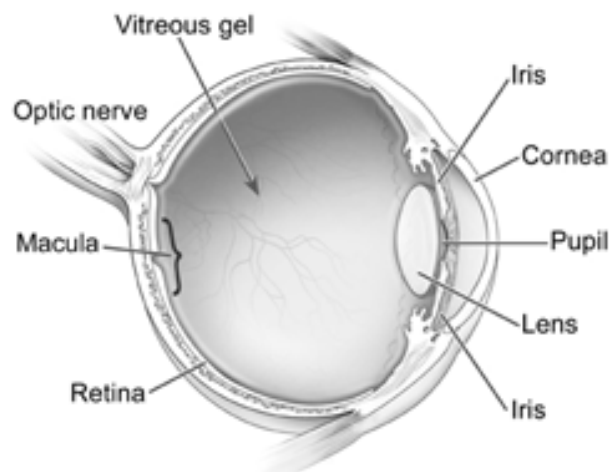


Figure. 1 –The anatomy of the eye [2]

In recent years, several eye diseases have become prevalent in the United States. Blindness or low vision affects 3.3 million Americans age 40 and over, and this figure is projected to reach 5.5 million by the year of 2020. Among various vision-threatening eye diseases, there are four primary types, which include cataract, glaucoma, age-related macular degeneration (AMD), and diabetic retinopathy, all of which may lead to irreversible blindness. [1]

One common ground of the primary eye diseases is that the focus of the disease is located at the posterior segment of the eye, which restricts effective treatment. Cataract is a clouding of the lens in the eye that affects vision. Glaucoma is a group of diseases that damage the optic nerve and result in vision loss and blindness. The reason for appearance of glaucoma is still ambiguous, but is believed that eye pressure may play an important role in damaging the optic nerve. Age-related macular degeneration is a disease associated with aging that gradually destroys sharp, central vision. There are two types of AMD, wet AMD and dry AMD, involving abnormal development of blood vessels and light-sensitive cells at the retina, respectively. Diabetic retinopathy is the most common diabetic eye disease, also caused by changes of blood vessels in the retina.

1.2 Current Treatment Strategies for Eye Diseases

The success of therapy to eye diseases, strongly depends on achieving sufficient drug concentration at target tissue for a sufficient period of time. However, for most eye disorders located at the posterior segment of the eye, controlled drug delivery is a major challenge due to the need to overcome physiological barriers.

Generally speaking, there are two ways for ocular drug delivery, systemic administration and topical administration. The former has been used to treat a few vitreo-retinal diseases, such as glaucoma [3] and dry eye [4]. However, a previous study showed that only limited quantities of about 1-2% of drug could be distributed to the eye. [5] The limitations are due to the blood-retina barrier, which is selectively permeable for hydrophobic molecules and prevents drugs from reaching the posterior segment of the eye. As a result, large doses are required to obtain sufficient drug concentration at the target sites, leading to significant peripheral side effects. On the other hand, drug administration in a topical route is preferred due to the ease of administration, as well as low cost.

Non-invasive treatments include eye drops, ophthalmic gels, ointments, and contact lenses. More than 90 % of the marketed ophthalmic formulations are in the form of eye drops. Conventional eye drops are easily eliminated at the precorneal area due to tear drainage and blinking, and actually less than 5% amount of drug can reach the posterior segment of the eye. Besides, eye drops provide a pulse entry of the drug, followed by a rapid decline in drug concentration. In other words, dosage via eye drops is inconsistent and difficult to regulate, rendering most of the drug released in an initial burst. In addition, the remainder of drug is drained into the nasal cavity, where the drug is then absorbed into the bloodstream. This leads to an extensive systemic absorption and may result in undesirable side effects. As an example, timolol ((*S*)-1-(*tert*-butylamino)-3-[(4-morpholin-4-yl-1,2,5-thiadiazol-3-yl)oxy]propan-2-ol, a beta blocker) in form of eye drops can slow the heart for at least the first six months of use. Ophthalmic gels and ointments are semisolid dosages developed with increased viscosity in order to prolong

the retention time of the drug at the precorneal area, and thus improve bioavailability. However, they may blur the vision significantly. Contact lenses have been used for ophthalmic drug delivery, because they provide a much longer residence time in the tear film, thereby results in higher drug flux through the cornea and reduce the drug elimination through bloodstream in the nasal cavity.

Invasive treatments, such as intravitreal injections or implants provide efficient drug delivery to the back of the eye, as well as reduced systemic toxicity. Frequent administration of drug via injection results in extreme patient discomfort and may cause retinal detachment, infections, and vitreous hemorrhage. [6] The long-term accumulation of intravitreal implants might significantly impact the patient's vision. [6]

1.3 Controlled Drug Delivery Systems

Although the conventional dosage forms, such as eye drops or ointment, are not cost efficient to treat posterior segment diseases, noninvasive topical administrations may have advantages in reducing side effects, easy application and good compliance. Therefore, novel drug delivery systems like nanoparticles/nanosuspensions, hydrogel, particle-embedded contact lenses, and dendrimers have been developed for this purpose.

The noteworthy impact of controlled drug delivery systems is that the limitations of conventional delivery systems in ocular drug delivery and different barriers present inside the eye can be successfully overcome. Controlled drug delivery systems maintain the drug in the desired therapeutic range by a single administration, and offer selective targeting at the desired site, thus increase the efficiency of drug delivery by improving the release profile and also reduce drug toxicity. Ocusert, one of the earliest clinically

used controlled release systems was designed to improve the therapy of glaucoma. The Ocusert delivers pilocarpine ((3*S*,4*R*)- 3-ethyl- 4-((1-methyl- 1*H*-imidazol- 5-yl) methyl)dihydrofuran- 2(3*H*)-one) continuously for one week with less drug and fewer side effects. [7] In previous work by our research group, a thin membrane embedded with drug-loaded nanoparticles was characterized. The *in vitro* drug release test showed a sustained release for seven days.

For an excellent controlled drug delivery system for ophthalmic administration, the following properties are desirable. i) Extended residence time, to prolong the contact time of the drug delivery system at the preconeal area. ii) Improved solubility, to facilitate parenteral drug administration. iii) Targeting, to increase the drug concentration at targeted tissues and reduce systemic drug levels. iv) Controlled drug release, to maintain a constant therapeutic dose at the function site. v) More convenient routes of administration. vi) Nanoscale, to avoid any uncomfortable feelings and improve compliance.

1.4 Development of a Novel Ophthalmic Drug Delivery Device

For the present work, we propose a design of drug loaded core-shell nanoparticles as shown in Fig. 2. Lidocaine, a hydrophobic small molecular drug, was selected as the model drug, due to its representativeness of many ophthalmic drugs. Core nanoparticles are synthesized with PGA, since it is biocompatible, biodegradable, and with good potential for long-term drug delivery. With lidocaine loaded within polyglycolide cores, the shell was constructed by alternative deposition with negatively charged type I collagen and positively charged chitosan, The alternative coating, also called LbL self-

assembly, is a promising way to produce multilayers with controllable thickness, which renders controllable sized nanoparticles. The alternative deposition will be repeated for three times to obtain three bilayers, and chitosan was designed as the outmost layer due to its advantageous mucoadhesive property that provides longer residence time at the precorneal area. Type I collagen, the most abundant protein in human body, is selected because it is biocompatible and weakly biodegradable. These core-shell nanoparticles are suitable for dry storage, and can be easily resuspended in aqueous fluid before administration.

The resulting nanoparticles were characterized. The size distribution was measured to show appropriate average size and deviation within nanoscale. SEM images were taken to confirm the size distribution, as well as to show the morphology of the nanoparticles. FTIR spectra indicated successful entrapment of model drug within core nanoparticles. A variation of zeta potential after each coating cycle confirmed layer growth and gives a reference of the colloidal stability of nanoparticles in suspension. Finally, *in vitro* drug release was measured over a period of 20 days.

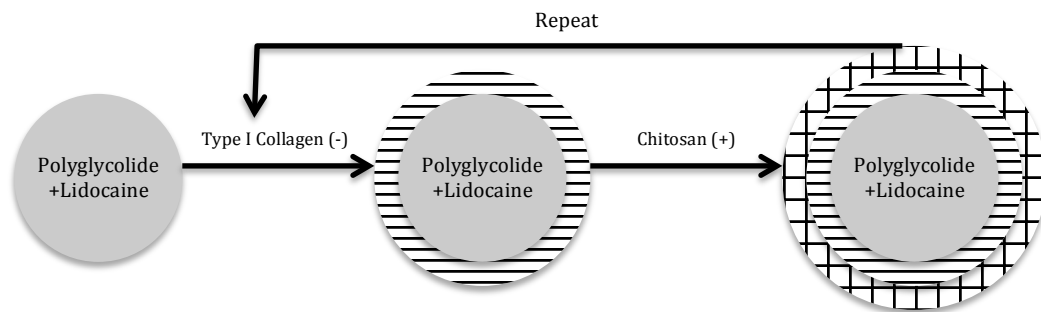


Figure. 2 – Details of novel ophthalmic drug delivery device

CHAPTER II

LITERATURE REVIEW

Despite years of effort by many scientists and engineers, the delivery of ocular drug by penetrating through a few barriers is still a challenge. Most chronic eye disorders are treated topically with drug in the form of conventional solutions, suspensions, and ointment. Administration of drug in this form suffers from rapid elimination and low bioavailability, due to the unique physiological structure of the eye. The main objective of this work is to develop an improved ocular drug delivery system to not only overcome solubility problem of hydrophobic drugs and drug targeting issues, but also with good mucoadhesive properties and controlled drug release profile.

2.1 Anatomy of the Eye

The eye is one of the most complicated organs in human body with many parts working for sense of sight. The eye is composed of the following two segments: (1) the anterior segment, which includes the cornea, iris, pupil, and lens, and (2) the posterior segment, which includes the vitreous body and retina. The main parts of the eye are shown in Fig.

1, and functions of each part are introduced as follows.

i. **Tear film** is the outmost part of the eye and is comprised of the following three layers: oil, water, and mucous. The lower mucous layer acts as tape, helping the tear film adhere to the eye. The upper oil layer prevents water evaporation. The tear film keeps the eye moist, creates a smooth surface for light to pass through the eye, nourishes the anterior segment of the eye, and protects the eye from injury and infection from exterior environment.

ii. The **cornea** is a transparent part in front of the eye that covers the iris, pupil, and anterior chamber. It contains no blood vessels, and receives nutrients via diffusion from outside tear liquid and inside aqueous humor.

iii. The **pupil** is a hole located in the center of the iris of the eye that allows light to enter the retina. It appears black because most of the light entering the pupil is absorbed by interior tissues.

iv. The **iris** is a thin, circular structure in the eye that is capable for controlling the diameter and size of the pupils by contracting or expanding the attached muscles, and thus to adjust the amount of light reaching the retina.

v. The **lens** is a transparent, biconvex structure in the eye. By changing shape it can accommodate the focal distance of the eye, and help to form a sharp image of the object of interest on the retina.

vi. The **vitreous humor** is a transparent gel-like liquid that fills up the space between the lens and the retina. The vitreous humor consists of very few cells and no blood vessels.

Although 98-99% of its volume is water, the vitreous humor serves to maintain the spherical shape of the eye.

vii. The **retina** is a light sensitive tissue that lines the inner surface of the eye. When light reaches the retina, it initiates a series of chemical and electrical impulses that trigger nerve signals that are sent to brain via the optic nerve.

viii. The **macula** is an oval-shaped pigmented yellow spot at the center of the retina. It is capable to absorb excess blue and ultraviolet light that enters the eye, and help to protect the eye as a natural sunblock.

ix. The **optic nerve**, located at the back of the eye, is a bundle of more than one million nerve fibers. It is used to transmit information from the retina to the brain. Its primary function is to relay electrical impulses to form images.

As shown in Fig. 3, the eye is partially isolated from the other parts of the body, as well as the environment by the following types of barriers: i) muco-aqueous layer of tear film, ii) the conjunctival and corneal epithelium, iii) the iris blood vessels, iv) the blood-aqueous barrier, and v) the blood-retina barrier.

The barriers described above make the eye highly defensive to foreign substance, and drugs are no exception. Drugs are mainly eliminated from the precorneal lacrimal fluid by solution drainage, lacrimation and nonproductive absorption to the conjunctiva of the eye. [8] For example, blinking and tear drainage through lachrymal drainage system remove topically applied drug within 30 seconds. The drug transport through corneal epithelium is essentially via paracellular or transcellular route. Hydrophilic drugs penetrate mainly through the paracellular pathway while hydrophobic drugs prefer the

transcellular route. Other factors, including solubility, molecular weight, shape, charge, and degree of ionization, also affect the route and rate of penetration through cornea. [8] Particulate nanocarriers have been reported to follow the endocytic pathway. [9] One of the maintenance strategies of the corneal transparency can be tight cell junction, which renders the interior part of the eye nearly impermeable to any macromolecules larger than 500 Da. [10]

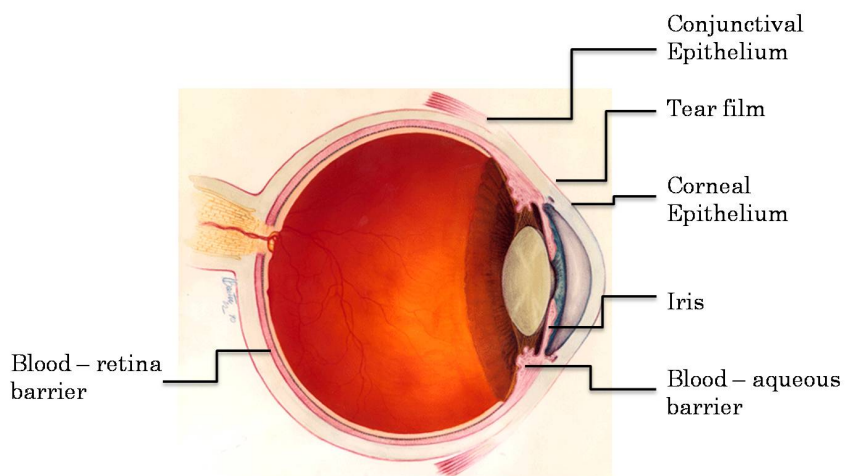


Figure. 3 –Physiological barriers of the eye [2]

2.2 Controlled Ocular Drug Delivery

Controlled drug delivery to the eye is one of the most challenging fields of ophthalmic research. Low drug-contact time and poor bioavailability due to precorneal elimination are problems associated with conventional systems. In addition, anatomical barriers and physiological conditions of the eye also confine effective topical drug delivery. Therefore,

novel drug delivery systems like nanoparticles/nanosuspensions, hydrogel, drug-loaded contact lenses, and dendrimers have been developed for this purpose.

2.2.1 Ophthalmic Hydrogels

In order to avoid the rapid dilution and elimination, eye drop formulations with an increased viscosity have been developed. Hydrogels are three-dimensional hydrophilic macromolecular networks containing large amount of water within their structure. The soft, insoluble properties are similar to natural tissue, which leads to wide applications in biomedical and pharmaceutical area. These formulations may contain various viscosity enhancing agents, such as poly(vinyl alcohol), poloxamer (a series of nonionic triblock copolymers), methyl cellulose, and carbopol (prop-2-enoic acid), and the drug is generally loaded throughout the formulation.

The drug release from hydrogel systems follows three mechanisms, diffusion control, chemical control, and swelling control. In diffusion-controlled systems, the drug can be dissolved or dispersed in the polymer, and then diffused driven by a gradient in thermodynamic activity. In chemical-controlled systems, the therapeutic agent is released by hydrolysis or enzymatic degradation of the polymer. In swelling-controlled systems, the influx of water in the hydrophilic polymer matrix and consequent swelling of the system controls the release of the drug. [11] The use of hydrogel in ocular topical administration can provide an enhanced bioavailability of drug as the residence time is significantly prolonged.

Gelation of hydrogels can occur when stimulated by environmental factors like temperature, pH and ionic strength. The in-situ gelling system is a free flowing liquid at

room temperature, allowing easy drop-wise administration into the eye. Upon exposure to physiological environments, the gel will undergo phase transition from liquid to a semisolid gel, which increases the mechanical strength of the system. Both thermosensitive polymers like poloxamer, and pH sensitive polymers like carbopol have been employed to develop in-situ gelling systems. [12]-[14] Mansour *et al.* [15] developed poloxamer-based in-situ gelling formulations of ciprofloxacin hydrochloride. The sol-gel transition temperature ranged from 28.00 to 34.03 °C, and the prepared formulae showed improved ocular bioavailability compared with the marketed conventional eye drops. Wu *et al.* [16] designed an in-situ pH triggered gelling system to improve the stability and bioavailability of baicalin, an anti-inflammatory and anti-cataract drug. Carbopol 974P was used as the gelling agent, and sol-gel transition occurred at pH 6.0. The formulation provided sustained release over eight hours. Gupta *et al.* [17] employed chitosan (a pH-sensitive polymer) in combination with gellan gum (an ion-activated polymer) to develop a gelling system. The gelation required pH 6.5 to 7.0 and osmolarity of 298 to 302 mOsmol, which is very close to physiological conditions.

With improved mechanical and mucoadhesive properties, the ophthalmic gels can prolong the retention time of the drug at the precorneal area, and thus improve bioavailability. However, gels may blur the vision. For some pH sensitive polymers, such as carbopol, an acidic pH is required before phase transition. This formulation may cause irritation to the eye tissue, and increases lacrimal secretion, which drains the formulation more quickly. [14]

2.2.2 Nanoparticles

During past decades, research on nanotechnology has gained extensive concerns, and has been applied in various biomedical areas, such as drug delivery, gene therapy, and diagnostics. With applications of nanotechnology in drug delivery systems, hydrophobic drugs, peptides, and proteins, can be delivered precisely to targeted sites.

Properly formulated drug loaded nanoparticles (DNPs), such as a colloidal system, can be a promising approach for ophthalmic drug delivery. A colloidal system is suitable for drugs with poor solubility in water. Dispersion of DNPs in a suitable solvent provides an easy dropwise application in liquid form just like regular eye drops. DNPs in eye drops can avoid discomfort associated with administrations of viscous or sticky preparations, such as ointment, which leads to blurry visions. Furthermore, it is possible for the particles to be retained in the ocular cul-de-sac for extended duration after topical administration, as well as sustained drug release. This makes DNPs more patient friendly as an additional advantage.

Nanoparticles with sub-micron properties differ from macroscopic objects in several aspects, such as high surface area to volume ratio, energy, and Brownian motion in liquid media. The reduced size of the particles helps with the adsorption and permeation through the ocular barriers. The reduced size also ensures patients will not experience abrasion to their eyes. There are many factors that have an influence on the drug release and degradation of the nanoparticles, including the size, morphology, physical state of the encapsulated drug, and molecular weight and crystallinity of the polymer. Measuring Zeta potential of the particles provide information about the surface charge, which

determines the stability of the colloidal system. Adequately high zeta potential values beyond +/- 30 mV are considered to be a stable colloidal dispersion.

Biodegradable nanoparticles for pharmaceutical use can be prepared from various synthetic and natural polymers. Some synthetic polymers are like polyacrylates, poly(lactide-co-glycolide), and polycaprolactones. Pignatello *et al.* [18] developed flurbiprofen (FLU) loaded acrylate polymer nanosuspensions for ophthalmic application. The incorporation of drug in the polymer nanoparticles enhanced FLU the availability at an intra-ocular level for the prevention of the myosis induced during extracapsular cataract surgery. Gupta *et al.* [20] developed a colloidal system with sparfloxacin (a newer-generation hydrophobic fluoroquinolone used in bacterial conjunctivitis) loaded PLGA nanoparticles to improve precorneal residence time and ocular penetration. Lacoulonche *et al.* [21] investigated the stability and in vitro release of FLU loaded poly- ϵ -caprolactone nanospheres. Natural polymers including albumin [24], alginate, gelatin [26], and chitosan [27] have also been used as nanocarriers. Kang *et al.* [25] reported a study on in vitro release of FITC-dextran (a dye, Mw 40,000) from alginate beads. They found that amaranth (a deep red dye) could be released for six hours with a first order profile. Wu *et al.* [28] were able to develop chitosan nanoparticles with excellent capacity for ammonium glycyrrhizinate, and the in vitro release test showed an obvious burst followed by a slow and continuous release phase.

Particle fabrication techniques include precipitation/coacervation, spontaneous emulsification/solvent diffusion, salting out/emulsification-diffusion, ionic gelation, and desolvation. Kakran *et al.* [30] prepared artemisinin ((3R,5aS,6R,8aS,9R,12S,12aR)-octahydro-3,6,9-trimethyl-3,12-epoxy-12H-pyrano[4,3-j]-1,2-benzodioxepin-10(3H)-one,

ART) nanoparticles by the precipitation method. Original ART powder was dissolved in a good solvent (ethanol), and then nanosuspension was formed by quickly adding an antisolvent (hexane). Then nanoparticles were recovered by evaporating the good solvent and antisolvent. El-Shabouri [31] reported chitosan NP preparation by the emulsification/solvent diffusion method. An oil-in-water emulsion was obtained upon injection of an organic phase into chitosan solution containing a stabilizing agent under mechanical stirring, followed by high-pressure homogenization. The emulsion was then diluted with a large amount of water, whereupon polymer precipitation occurs as a result of the diffusion of organic solvent into water, leading to the formation of nanoparticles. This method is suitable for high drug entrapment of hydrophobic drugs. The major drawbacks of this method are harsh processing conditions (e.g., the use of organic solvents) and the high shear forces used during nanoparticle preparation. Janes, *et al.* [32] fabricated doxorubicin (DOX) loaded chitosan nanoparticles by ionic gelation. The mechanism is based on electrostatic interaction between positive charge amine group of chitosan and negative charge group of a polyanion. DOX was first incubated with tripolyphosphate (a polyanion), and then added to a chitosan solution with acetic acid. Nanoparticles were formed upon mechanical stirring at room temperature. This process is simple with mild condition. Jun *et al.* [33] developed protein loaded bovine serum albumin (BSA) nanoparticles with the desolvation method. Protein and BSA were dissolved in an aqueous solution and stirred. A desolvating agent, acetone, was added dropwise to the stirring aqueous solution, thereby forming the nanoparticles.

2.2.3 Dendrimers

Dendrimers are macromolecular compounds made up of a series of branches around a central core [36], and the drug payload can be physically entrapped within the dendrimer or chemically attached to the surface [37]. Dendrimers can deliver drug with better water-solubility, bioavailability and biocompatibility and have successfully explored for different routes of drug administration. Poly(amidoamine) (PAMAM) dendrimers for delivery of pilocarpine nitrate and tropicamide (*N*-ethyl-3-hydroxy-2-phenyl-*N*-(pyridin-4-ylmethyl) propanamide) were developed by Vandamme and Brobeck [38]. They found that residence time was longer for the solutions containing dendrimers with carboxylic and hydroxyl surface groups. In another study, Yao *et al.* [39] prepared and evaluated puerarin (one of several known isoflavones) -dendrimer complex as an ocular drug delivery system. Puerarin-dendrimer led to longer residence time in rabbits compared with puerarin eye drops.

2.2.4 Drug-loaded Contact Lenses

Contact lenses have been used for ophthalmic drug delivery. Traditionally used soaked contact lenses provide a drug release for a few hours. Current challenges in this mode of drug delivery are to sustain release for longer period and also to incorporate sufficient drug amounts in the lens matrix. Lens provides a much longer residence time in the tear film, thereby results in higher drug flux through the cornea and reduce the drug elimination through bloodstream in the nasal cavity.

One type of soft contact lens can absorb a number of drugs when presoaked in the drug solution, and then release them into the post-lens lacrimal fluid. Alternatively, soft

contact lenses can be placed into a patient's eyes then drug-containing eye drops are applied. The drug can be absorbed and released by the soft contact lens, minimizing clearance and sorption through the conjunctiva. [40]

However, soft contact lenses do come with some disadvantages. For one, the content of drug loading by presoaking lenses in the drug solution is limited. [40] Therefore, lenses can only deliver drugs for a few hours. The residence time of a system could be lengthened by suspending nanoparticulate based drugs in contact lenses, which is similar as Mr. Sharma's design of nanoparticle embedded membrane. Another limitation is that it requires patients to wear the contact lens at all times. [41]

2.2.5 Implants

Ocular implants provide a platform for sustained release of molecules from either biodegradable or non-biodegradable polymeric matrices over several months to years. The implants can either be deposited into the vitreous body or sutured on the sclera as shown in Fig. 4. For example, Alginate coated implants of growth factors (epidermal) showed promising applications in ocular therapy of keratitis sicca. [42]

The design of implants involves drug solubility, diffusion coefficient of the drug in the polymer, drug loading capacity, and the degradation rate of the polymer.

Biocompatibility is essential to all components, which are required to be chemically inert, noncarcinogenic, hypoallergenic, and mechanically stable at the implantation site.

Although the ophthalmic implants are able to provide sustained release of drug, the high-density formulations deposited on the inferior retina may lead to local adverse

effects. In addition, the long-term accumulation of intravitreal implants might significantly impact the patient's vision. [6]

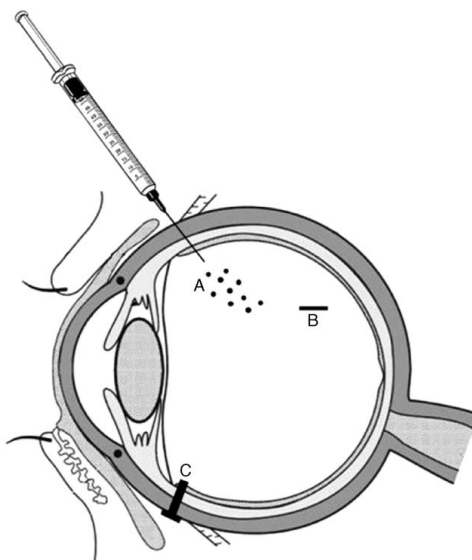


Figure. 4 –Schematic presentation of intravitreal route of drug delivery to posterior chamber of the eye. (A) Intravitreal injection through a needle. (B) Biodegradable or non-biodegradable implants introduced into the vitreous body. (C) Scleral plugs or implants sutured onto the sclera. [6]

2.3 Layer-by-Layer Assembly for Drug Delivery

Layer-by-Layer (LbL) assembly is an approach to construct a multilayers, by consecutive deposition of complementary and interacting polymers onto some template, taking advantage of interlayer force as shown in Fig. 5. The template can be particles, planes, tubes, and any irregular shapes. [43] Zheng *et al.* [44] made polyelectrolyte-coated

nanoparticles with curcumin ((1E,6E)-1,7-Bis(4-hydroxy-3-methoxyphenyl)-1,6-heptadiene-3,5-dione) crystal as a template. The drug release sustained up to 20 hours. Various materials can be used in self-assembly, including polymers, biomaterials, and inorganic species, and various interlayer forces can be employed when building multilayers. Electrostatic interaction, hydrogen bond, covalent bond, metal coordination, and bio-specific recognition have already been demonstrated successfully. Zhou *et al.* [45] deposited two natural polysaccharides, chitosan and alginate, by LbL assembly on PLGA nanoparticles for antifouling protection. The deposition was based on electrostatic interaction between the two polymers. Uttam *et al.* [46] constructed LbL assembly based on hydrogen bonding between DNA base pairs (adenine and thymine). Chitosan modified with adenine interacted with hyaluronic acid modified with thymine. Mu *et al.* [47] fabricated multilayer microcapsules via covalent LbL assembly. The covalent bonding occurred between the amino groups of chitosan and the aldehyde groups of oxidized sodium alginate. Wanunu *et al.* [48] achieved LbL growth of multilayer via metal-organic coordination using Zr^{4+} ions. Hoshi *et al.* [49] prepared thin films by LbL deposition taking advantage of a strong bioaffinity between concanavalin A (a carbohydrate-binding protein) and sugar chains attached to the surface of avidin (a biotin-binding protein). Among different strategies, covalent crosslinking has the best stability.

The capability of successive layer growth gives a freedom in both the number of layers and layering sequence. For different situations, variation of the shell thickness within 20 to 100 nm allows the release time to vary from several minutes to a few weeks. Ye *et al.* [51] were able to construct thickness about 13 nm and five bilayers of chitosan and

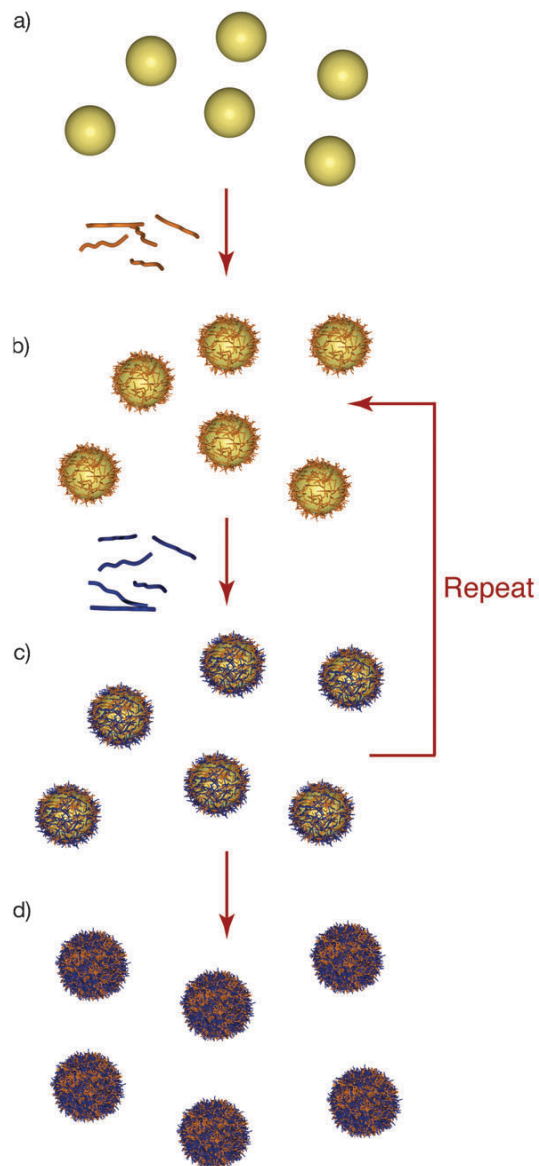


Figure. 5 - Layer-by-Layer (LbL) assembly of polyelectrolytes on particles. (a) Particles with an inherent charge are incubated in a solution of oppositely charged polyelectrolytes. (b) Following centrifugation/ rinsing steps to remove excess polyelectrolyte, the coated particles exhibit charge reversal, which facilitates the adsorption of another layer of oppositely charged polyelectrolyte. (c) The process is repeated until the desired number of layers/ thickness is achieved. (d) The particle templates can be subsequently removed to yield polyelectrolyte capsules. [50]

sodium alginate on monodisperse polystyrene, and obtained a sustained release of acridine hydrochloride (a hydrophilic drug, Mw 215.68) up to five hours.

The construction of multilayers in an LbL manner has several favorable features. First, the surface properties may be tailored by selecting materials suitable for specific purposes. For example, to use a positively charged material as the outmost layer will offer better mucoadhesive property, because the mucosa is negatively charged. [52] Second, the LbL assembly process is usually performed with simple operations in aqueous medium at room temperature, and does not require harsh conditions. Therefore, it becomes possible to apply biomaterials, such as polysaccharides and proteins without changing the chemical structure or specific bioactivity.

2.4 Selection of Biodegradable Polymers

2.4.1 Core Material

Polyglycolide (PGA) is a linear, semi-crystalline aliphatic polyester, as shown in Fig. 6. It is non-toxic and biodegradable in the human body, and has good mechanical strength. Consequently, this polymer has found many applications in the biomedical area, such as a wound closure material, a surgical suture, and a tissue engineering scaffold. Previous research also revealed its potential in drug delivery. Hurrell and Cameron [53] developed a drug-loaded 3D matrix by incorporating a small molecule hydrophobic model drug, theophylline (a small hydrophobic drug, Mw 180.16), into polyglycolide, and reported a sustained release for 20 days.

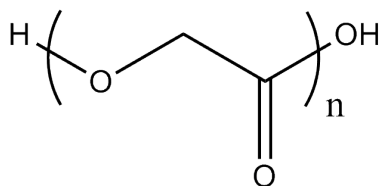


Figure. 6 – Chemical structure of polyglycolide

The degradation of PGA is a complicated process. Generally, it degrades in the presence of water by a hydrolysis reaction at the ester backbone, which is acid catalyzed and reversible. Hurrell and Cameron [54] proposed a four-stage reaction-erosion front model. In stage I, which occurs over the first a few hours after immersion, water diffuses into the polymer matrix homogeneously and scission of the chains by hydrolysis begins as the polymer contacts water. During stage II, little water is absorbed and subsequent hydrolysis of the polymer continues. During this stage very little mass is lost, because the chains are still too large to diffuse from the polymer matrix. In stage III, some oligomers are small enough to dissolve into the media, and a reaction-erosion front forms, separating the central autocatalyzing region from the surface where the oligomers diffuse out. As oligomers escape, space is created to allow for more water to come in, drug is released rapidly, and the reaction-erosion front moves towards the sample center. At the beginning of stage IV, the front meets the sample center, and drug release is completed. Fig. 7 shows drug release for the four-stage degradation process.

Although polyglycolide shows a convenient timescale of degradation, is semi-crystalline in nature, biocompatible, and excellent drug loading efficiency, it is seldom investigated to fabricate drug-loaded nanoparticles due to its difficulty in handling.

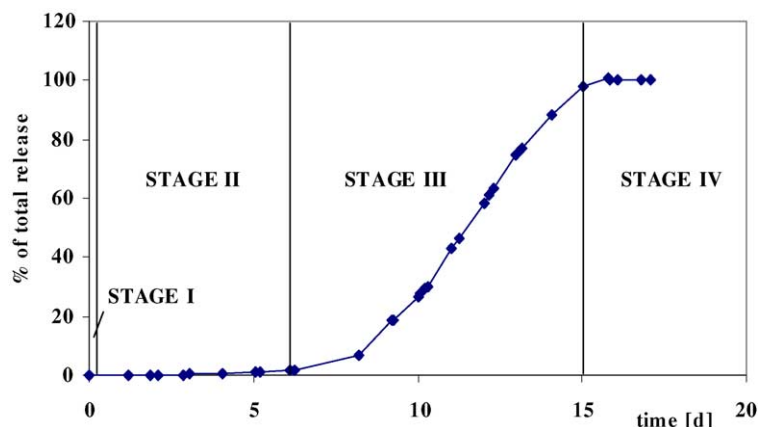


Figure. 7 – The relationship between drug release and the four-stage degradation process [55]

2.4.2 Shell Material – Type I Collagen and Chitosan

Desired shell properties include good biocompatibility, as well as good mucoadhesive property. The following two oppositely charged, biodegradable materials were chosen to fabricate the shell by the layer-by-layer method: type I collagen and chitosan.

Collagen is composed of a triple helix, which generally consists of two identical chains and an additional chain slightly different in its chemical composition. Type I collagen is the most abundant protein present in mammals. Collagen is the major component of the extracellular matrix and serves as a natural substrate for cell attachment. Consequently, collagen has been widely used for wound dressing, which was approved by the US Food and Drug Administration (FDA). Collagen undergoes enzymatic degradation within the body via enzymes, such as collagenases and metalloproteinases, to yield corresponding amino acids. Fathima *et al.* [59] tested the degradation time of collagen fibrils in vitro at

37°C and treated with collagenase, which took 96 hours for 96% weight loss. They also found that native collagen underwent a hydrothermal shrinkage at 62 ± 1 °C. Rudakova and Zaikov [60] studied degradation of collagen thread in aqueous H₂SO₄ and KOH solutions. Obscure weight loss occurred at 40 °C and above in 0.1 N H₂SO₄, and at 30 °C and above in 0.1 N KOH. Without being treated with enzymes, thermal heat, and strong acid or alkali, collagen is quite stable in aqueous solutions. Collagen is an electrochemically inert protein with an isoelectric point at 5.5, which means it carries a net negative surface charge at pH 7.0. Some researchers take advantage of this property, and fabricate layer-by-layer films with collagen. Miao *et al.* [61] assembled collagen with electroactive myoglobin into layer-by-layer films on solid surfaces. They treated the solid template alternately with collagen aqueous dispersions and myoglobin solutions (pH 5.0, since isoelectric point for myoglobin is 6.8). UV-Visible light spectroscopy and cyclic voltammetry was used to confirm the film growth. Also, the thickness of the collagen film was investigated. Zhang *et al.* [62] estimated the type I collagen film as 20-30 nm for collagen/ hyaluronic acid film by Atomic force microscopy (AFM).

Chitosan is a linear polysaccharide and non-toxic in oral administration approved by FDA. Chitosan has a similar degradation pattern to that of collagen, and undergoes enzymatic hydrolysis in vivo with enzymes, such as lysozyme. A study showed that it took one to two months for chitosan microparticles (500 ± 150 µm) to degrade completely in vitro at 37°C and treated with lysozyme and NAGase. [63] When dissolving in weak acidic solutions, chitosan is charged with a high density of cations, which provides it with potential in layer-by-layer fabrication. The strong positive charge

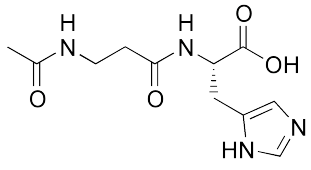
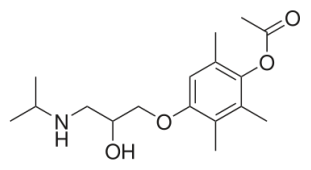
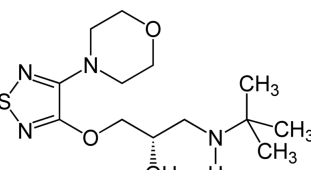
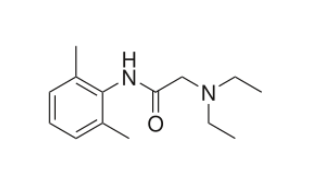
also makes chitosan as a quite effective mucoadhesive polymer due to strong interaction with a negatively charged mucous membrane. [64]

2.5 Selection of Model Drug

Many ophthalmic drugs have chemical properties in common. As shown in Table. 1, N-acetylcarnosine (NAC) for treating cataract, metipranolol and timolol for treating glaucoma, lidocaine for ocular surface anesthesia, are all small molecules drugs with poor solubility in water. This makes them difficult to be delivered by using aqueous eye drops. To achieve better solubility, the molecules need to be conjugated with acids to form salts. For example, metipranolol hydrochloride and lidocaine hydrochloride are hydrophilic, thus easily soluble in water. But for some cases where conjugation is not available, or the drug efficacy is compromised due to the conjugation, the drug will not be able to deliver in forms of conventional eye drops.

Lidocaine was selected as the model drug in this research based on its physical and chemical properties. Its formula is $C_{14}H_{22}N_2O$, and molecular weight is 234.24 g/mol. Lidocaine was first synthesized by a Swedish chemist Nils Löfgren in 1943, and is used widely as a local anesthetic agent.

Table. 1 – Chemical structures of some ophthalmic drugs

Name	Chemical Structure	Molecular Formula	Molecular Weight
N-acetylcarnosine		$C_{11}H_{16}N_4O_4$	268.27
metipranolol		$C_{17}H_{27}NO_4$	309.40
timolol		$C_{13}H_{24}N_4O_3S$	316.42
lidocaine		$C_{14}H_{22}N_2O$	234.34

CHAPTER III

MATERIALS, EQUIPMENT AND METHODOLOGY

3.1 Chemical Reagents

Polyglycolide (PGA, Purasorb PG20, intrinsic viscosity midpoint 1.4 dl/g) was donated by Purac Biomaterials (Netherland). Purified bovine type I collagen solution (PureCol, 97% purity, 3.1 mg/ml, pH~2) was purchased from Advanced Biomatrix (San Diego, CA). Chitosan was purchased from FMC BioPolymer (Philadelphia, PA). Phosphate buffer saline solution (PBS, pH 7.4) was prepared from salt that that was purchased from Invitrogen (Grand Island, NY). 1, 1, 1, 3, 3, 3-hexafluoro -2-propanol (HFIP, $\geq 99\%$), and dimethyldidodecylammonium bromide (DMAB, 98%) were purchased from Sigma-Aldrich (St. Louis, MO). 2-diethylamino-N-(2, 6-dimethylphenyl) acetamide (Lidocaine, USP) was purchased from Spectrum (Gardena, CA). Acetonitrile (HPLC grade) and dichloromethane (HPLC grade) were purchased from Pharmaco (Brookfield, CT). Hydrochloric acid (36.5 - 38%) was purchased from EM Science (Gibbstown, NJ). Sodium hydroxide (99.2%) and sodium chloride (100.0%) were purchased from Fisher

Scientific (Fair Lawn, NJ). All chemicals were used as purchased. Water was type I ultrapure.

3.2 Equipment

Lindberg/Blue M Box Furnace, Fisher Scientific Thermix Stirring Plate Model 210T, Fisher Scientific Sonic Dismembrator Model 500 with 1/2" flat probe, RC5C Centrifuge from Sorvall Instruments from DuPont Corporation, Thermo Fisher Scientific Signature Ultra-Low Temperature Freezer, ATR FD 3.0 freeze dryer from Appropriate Technical Resources, Nalgene Oak Ridge Centrifuge Tubes (50 ml), Nalgene Cryo 1 °C Freezing Container, Brookhaven Zeta PALS (particle analyzer based on dynamic light scattering), FEI Quanta 600 Field Emission Gun Environmental Scanning Electronic Microscopy (SEM), Shimadzu UV-1201 UV-Vis Spectrophotometer, Perkin Elmer Spectrum System 2000 FTIR Spectrometer.

3.3 Synthesis of Lidocaine-Loaded Polyglycolide Nanoparticles

PGA was removed from refrigerator and allowed to stand for approximately one hour to come to room temperature. PGA was allowed to come to room temperature prior to opening in order to avoid any moisture that might accumulate on the cold powder due to condensation. As donated, the PGA is a semi-crystallized, hard solid with a slightly yellow and opaque color. Its elevated degree of crystallinity, around 45-55%, results in insolubility in most organic and inorganic solvents. To achieve solubility, PGA was heat treated to become amorphous. Since the melting point of PGA was reported at 227 – 230 °C, a furnace was heated by 10 °C/ min from room temperature to 235 °C and stabilized. PGA was placed in a stainless steel container and heated for two minutes to

melt, then immediately quenched with liquid nitrogen (approximately -80 °C). The heating process was limited to a short period to avoid thermal decomposition of the polymer. [76] The resulting amorphous PGA appeared yellow and transparent.

In this work, an emulsion-evaporation method was employed to fabricate drug-loaded nanoparticles. The process involves two solutions. An organic solution was prepared in a 50 ml amber sample bottle with cap to avoid possible heating up by sunlight, because the organic solvent is highly volatile. At room temperature, 100 mg of PGA and 500 mg lidocaine was dissolved in 40 ml HFIP and stirred on a stir plate for four hours to get a homogeneous solution. In a 300 ml beaker, 2000 mg DMAB was dissolved in 200 ml DI water and stirred for two hours to form a 1% w/v aqueous solution. Afterwards, the aqueous phase was placed on an ice-water bath with the tip of sonicator probe inserted half the liquid height. With sonication at 90% intensity (the max power is 400 w, 20 kHz), the organic phase was added dropwise with a pipette within one minute, thereby forming the nanoparticles. No additional time for sonication. The mixture was stirred for 10 hours to evaporate most of the organic solvent.

The suspension of nanoparticles was collected in six 50 ml centrifuge tubes, and centrifuged at 12,000 rpm at 4 °C for 20 minutes. The supernatant was substituted with 40 ml fresh DI water. The nanoparticles were re-suspended and centrifuged. The steps of rinse and centrifugation were repeated six times to remove DMAB. Finally, the nanoparticles were suspended in 15 ml fresh DI water and distributed evenly into 15 pre-weighed and pre-marked 2 ml vials. These vials were placed inside an isopropanol-jacketed container (Nalgene Cryo 1 °C Freezing Container) and deposited in an -86 °C freezer for ten hours. The container was used to freeze the suspension slowly at a rate of -

1 °C/min, which prevents unwanted agglomeration of the particles. The resulting frozen suspension of nanoparticles was lyophilized (freeze dried) for 12 hours with the freeze dryer. The dried nanoparticles in the vials were weighed and used for characterization, further layer-by-layer entrapment, and test of drug release.

3.4 Layer-by-Layer Assembly

Two oppositely charged polyelectrolytes were employed to build the shell layers.

Collagen solution was prepared by diluting Type I collagen in 0.5 M NaCl aqueous solution to get a concentration of 0.3 mg/ml. The solution was adjusted to pH ~ 8 with 0.1 NaOH (aq.) with stirring on an ice-water bath. At this pH, type I collagen carries a net negative charge, since it is a protein with isoelectric point at pH 5.5. [77] The ice-water bath was used to avoid gelation of the collagen solution. Chitosan was dissolved in a 0.5 M NaCl aqueous solution to get the same concentration of 0.3 mg/ml. A 0.1 M HCl (aq.) was used to adjust the chitosan solution to pH ~ 3 at room temperature. At this pH, chitosan was given a positive surface charge due to its pK_a value ~ 6.1. [78] The two solutions were stirred for two hours to ensure that they were well mixed.

Core nanoparticles (100 mg) were suspended in 30 ml of the collagen solution and deposited for 20 minutes without stirring to obtain the first layer. The resulting suspension was centrifuged at 12,000 rpm, 4 °C for 20 minutes. The supernatant was discarded and 0.5 M NaCl (aq.) was used to rinse the particles three times. The second layer was constructed by adding the particles to 30 ml of the chitosan solution for 20 minutes. The centrifugation and rinse process was the same as that for building up of the first layer. The negatively charged type I collagen and positively charged chitosan were

alternatively used to treat the particles. The layer-by-layer building steps were repeated six times to construct three bilayers on the nanoparticles. Finally, the resulting core-shell nanoparticles were rinsed with 40 ml DI water for six times, and lyophilized as mentioned for core particles.

3.5 Size Distribution

Four samples were prepared, including PGA core particles, PGA/(Col) cores with one layer of type I collagen, PGA/(Col/Chi) cores with one bilayer, and PGA/(Col/Chi)₃ core-shell particles with three bilayers. Each sample of the particles was prepared in aqueous solution at 0.01 mg/ml. In order to avoid agglomeration that may significantly affect the result, each sample was ultrasonicated with 10 % intensity for two minutes and measured immediately.

The size distribution of each sample was measured by dynamic light scattering (DLS), which is a non-invasive, well-established technique. One typical application of DLS is to determine the size distribution of small particles in suspension or polymers in solution. The principle is based on the fact that all particles, polymers, and small molecules in suspension undergo Brownian motion. If they are hit with a laser, the light will scatter in all directions, as long as the particles are smaller than the laser wavelength, and a time-dependent fluctuation of the intensity of the scattered light can be observed. The intensity fluctuation is dependent on particle size, because the smaller particles move more rapidly. Analysis of intensity autocorrelation function provides the diffusion coefficient of the particles, and the hydrodynamic radius is related by Stokes-Einstein Equation.

3.6 Morphology

The morphology of core particles and core particles with three bilayers was observed with SEM. Each sample was suspended in DI water, sonicated for 1-2 minutes, and immediately applied to a metal grid. The metal grid was air dried, and no gold sputtering was employed.

3.7 Fourier Transform Infrared Spectroscopy (FTIR)

As for other absorption spectroscopy (e.g. UV-Vis spectroscopy), the goal of FTIR is to measure how well a sample absorbs light at each wavelength. The difference is that this method uses a beam containing many different frequencies of light rather than a monochromatic beam. The test method also uses beams with different combinations of light frequencies to obtain interferogram due to wave interference. The test process is repeated for many times to gather raw data (light absorption) at each combination. To obtain the spectrum, a computer gathers and processes the data with a common algorithm called the Fourier transform.

FTIR analysis was performed on the samples of lidocaine and lidocaine-loaded PGA nanoparticles. Each sample was mixed with solid KBr to reach a concentration of approximately 10% by weight. The mixture was pressed to form a small round disk and examined from 4,000 to 600 cm^{-1} .

3.8 Zeta Potential

Zeta potential is a measurement of the magnitude of the electrostatic charge repulsion or attraction between particles, and is one of the fundamental parameters to affect stability.

For charged particles in a suspension, an interfacial double-layer structure is usually formed on the surface, as shown in Fig. 8. The first layer (stern layer) is compacted with ions of opposite sign from the surrounding solvents. Due to thermal motions of solvent molecules and ions, this countercharge stretches out for some distance thereby forming a loose second layer called diffuse layer. Zeta potential is the potential difference between the dispersion medium and the stationary layer of fluid attached to the dispersed particle. A value of ± 30 mV can be taken as the line that separates stable and unstable suspensions. Particles with zeta potential more positive than +30 mV or more negative than -30 mV are normally considered stable.

In aqueous media, the pH of the sample is one of the most important factors that affect its zeta potential. For the core particles, and all the nanoparticles with chitosan as the outmost layer, 10 mM KCl (aq., pH~3) was used to prepare the suspensions. For nanoparticles with collagen as the outmost layer, 10 mM KCl (aq., pH~8) was employed. This was done in order to show the stability of the particles during the fabrication process. Since oppositely charged polyelectrolytes were used alternatively to construct layers, a charge reverse was expected as the layer growth. Furthermore, the PGA core particles and core-shell particles with three bilayers PGA/(Col/Chi)₃ were also measured in PBS to show the stability in physiological conditions.

Samples were measured with Brookhaven ZetaPALS, which applies an electric field to a suspension and measures how fast a particle can move. This process is called electrophoresis. The larger the charge it carries, the faster the particle will move.

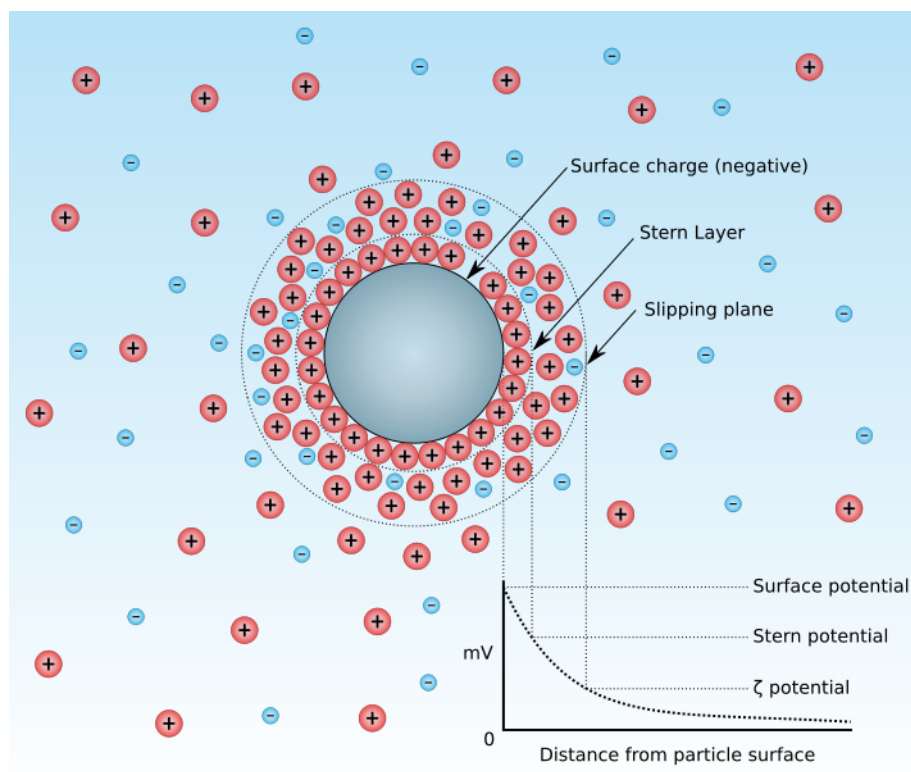


Figure. 8 – Diagram showing a double-layer structure on a negative charged particle surface [79]

3.9 Drug Loading

The amount of lidocaine loaded into the particles was determined by a UV-vis spectroscopy method. Since the particles contained several components, including lidocaine, PGA, type I collagen and chitosan, an appropriate wavelength was needed, at which lidocaine has the largest light absorption, while others do not. Aqueous solutions of lidocaine, type I collagen and chitosan were prepared separately at concentration of 0.1 mg/ml and scanned at wavelength from 200 nm to 400 nm, respectively. PGA is insoluble in water, thus not considered.

Standard solutions of aqueous lidocaine were prepared at several known concentrations and measured with UV-vis spectroscopy at the determined wavelength. A standard curve was set up by correlating the measured optical density subtracted by the blank control to the known concentration. The curve was used to determine drug loading and drug release by further interpolation.

Approximately 15 mg of each of PGA core particles, cores with one layer PGA/(Col), cores with one bilayer PGA/(Col/Chi), and core-shell particles PGA/(Col/Chi)₃ with three bilayers was treated with excess 2 M NaOH (aq.) while heating. The treatment was done to degrade the polymers, and form sodium salts with the degraded oligomers, thereby completely release the model drug. After 20 minutes, the earlier opaque suspension was observed to become transparent. The resulting solution was extracted with 2 ml dichloromethane. Since lidocaine is hydrophobic and other compounds are salts that are soluble in water, lidocaine can be distributed primarily in dichloromethane and separated from other components. The organic phase would be used to determine the lidocaine content by interpolating with the standard curve. And the drug loading content was calculated by the following equation.

$$\text{Drug Loading Content (\%)} = \frac{\text{Conc. Lidocaine} \times \text{Vol. solvent}}{\text{Mass particles}} \quad (3-1)$$

3.10 Drug Release Profile

Approximately 25 mg of each of PGA core particles, cores with one layer PGA/(Col), cores with one bilayer PGA/(Col/Chi), and core-shell nanoparticles PGA/(Col/Chi)₃ with three bilayers was suspended in 1 ml phosphate buffered saline (PBS) and incubated at 37 °C. At specified time intervals, each sample was centrifuged, supernatant collected,

and 1 ml fresh PBS was used to resuspend the particles. The following sampling time point were used for the study: 2, 4, 6, 8, and 10 hours for the first day and then once a day for the next 19 days. The UV absorbance was measured for the supernatants with subtraction of the blank control of PBS.

3.11 Statistical Methods

In the present work, several statistical methods were employed to process original data. For average particle diameter and standard deviation,

$$D_{avg} = \frac{\sum D_i N_i}{\sum N_i} \quad (3-2)$$

$$\sigma = \sqrt{\frac{1}{N} \sum (D_i - D_{avg})^2} \quad (3-3)$$

Where D_{avg} – nm, the average diameter of nanoparticles,

D_i – nm, an individual diameter of a group of nanoparticles,

N_i – dimensionless, the occurrence of each individual diameter,

N – dimensionless, the total occurrence,

and σ – nm, the standard deviation of the size distribution.

For drug loading contents, release samples and other samples with triplicates, similar statistical methods as Equation (3-1) and (3-2) were used.

CHAPTER IV

RESULTS AND DISCUSSION

4.1 Size Distribution

The hydrodynamic diameters were measured with Brookhaven Zeta PALS, and size distributions were given for each sample. As shown in Fig. 9, the distribution range for each sample was quite narrow ($\pm 2\%$). And the average diameters for the four samples were shown in Table. 2.

Table. 2 – Average diameters for four nanoparticle samples. Data are means \pm SD.

Sample	Average Diameter, nm
PGA	157.6 \pm 1.0
PGA/(Col)	186.3 \pm 1.7
PGA/(Col/Chi)	221.9 \pm 0.6
PGA/(Col/Chi) ₃	391.2 \pm 4.5

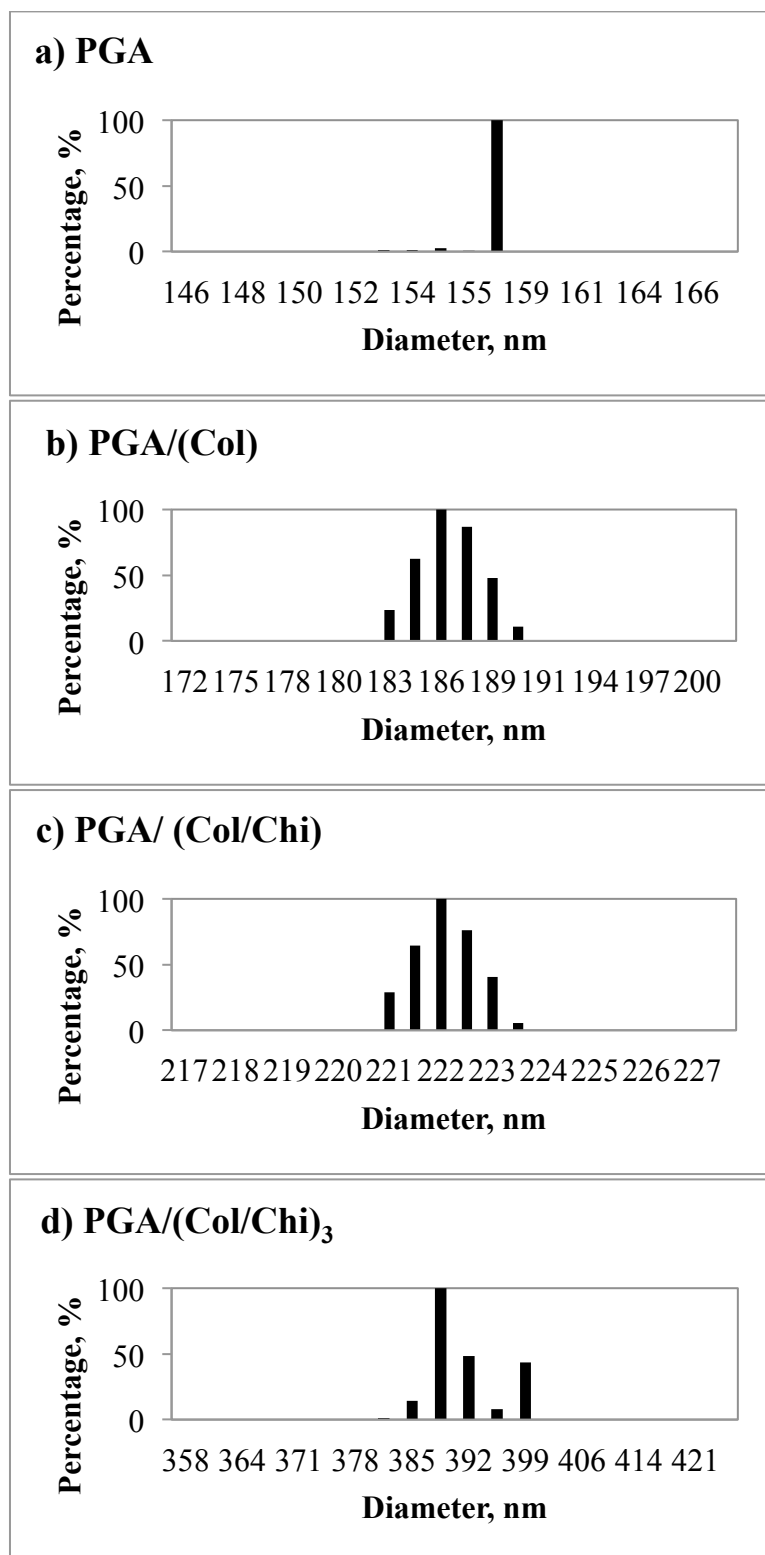


Figure. 9 – Hydrodynamic size distribution of a) – PGA core nanoparticles, b) – PGA/(Col), c) – PGA/(Col/Chi), and d) – PGA/(Col/Chi)₃

From these data, the thickness of each layer can be estimated. Two methods were used to estimate the thickness of each layer. One method is to subtract the two diameters and divided by 2 (accounts for symmetry) as follows.

$$Thickness_{collagen} = \frac{D_{PGA/(Col)} - D_{PGA}}{2} \quad (4-1)$$

$$Thickness_{chitosan} = \frac{D_{PGA/(Col/Chi)} - D_{PGA/(Col)}}{2} \quad (4-2)$$

By using the above method, the thicknesses of the collagen and chitosan layers are approximately 14.4 ± 1.4 and 17.8 ± 1.2 nm, respectively. The thickness of the bilayer was determined by adding the thicknesses of one single layer of collagen and chitosan and was determined to be approximately 32.2 ± 2.6 nm.

The other method to calculate the thickness of the bilayer is to subtract the core diameter measurement from the diameter of the core with three bilayers measurement and divide by three (accounts for three bilayers) and by two (accounts for symmetry). By using this method, the thickness of the bilayer was determined to be 39.0 ± 0.9 nm.

$$Thickness_{bilayer} = \frac{D_{PGA/(Col/Chi)} - D_{PGA}}{2 \times 3} \quad (4-3)$$

The two results vary by approximately 19% since the first method accounts for the thickness of the first bilayer, while the second method is based on an average thickness of the three bilayers. The difference indicates that the thicknesses for each bilayer is not uniform, Because the thickness of each layer is affected by many factors, including the surface charge of the particles, the concentration of polyelectrolytes, the concentration of NaCl, and the pH value of the solution. Although the latter three factors were maintained the same during the fabrication process, the surface charge was difficult to control.

4.2 Morphology

The morphology of core nanoparticles and core nanoparticles with three bilayers were obtained with an SEM. Fig. 10 shows that for both sample types, most of the particles are oval shape. Also, the SEM analysis was used to confirm the particle size. Fig. 10 Part (a) shows the morphology of core nanoparticles within some agglomerates. Some individual particles can be observed ranging from 100 to 200 nm as marked. The high intensity of the electron beam deforms the polymeric nanoparticles, resulting in large agglomerations, as shown at the bottom of the image. In Fig. 10 Part (b), thousands of core nanoparticles with three bilayers form large agglomerate, which indicates a poor stability, compared to that of the core particles. The diameter of some randomly measured particles ranged from 250 to 430 nm. Both images confirm the size distribution results with the previous results obtained by DLS.

4.3 FTIR

The successful entrapment of lidocaine within PGA was confirmed with FTIR spectra. Fig. 11 Part (a) shows the infrared spectrum of lidocaine with typical bands at 3283 cm^{-1} (N-H stretching), $2823 - 2970\text{ cm}^{-1}$ (C-H stretching), 1683 cm^{-1} (C=O amide), 1496 and 1594 cm^{-1} (aromatic C=C). When comparing the spectra in Fig. 10 Parts (a) and (b), there are obvious differences at 1215 cm^{-1} (C-O ester) and 1747 cm^{-1} (C=O ester), both of which indicate that lidocaine was incorporated with PGA.

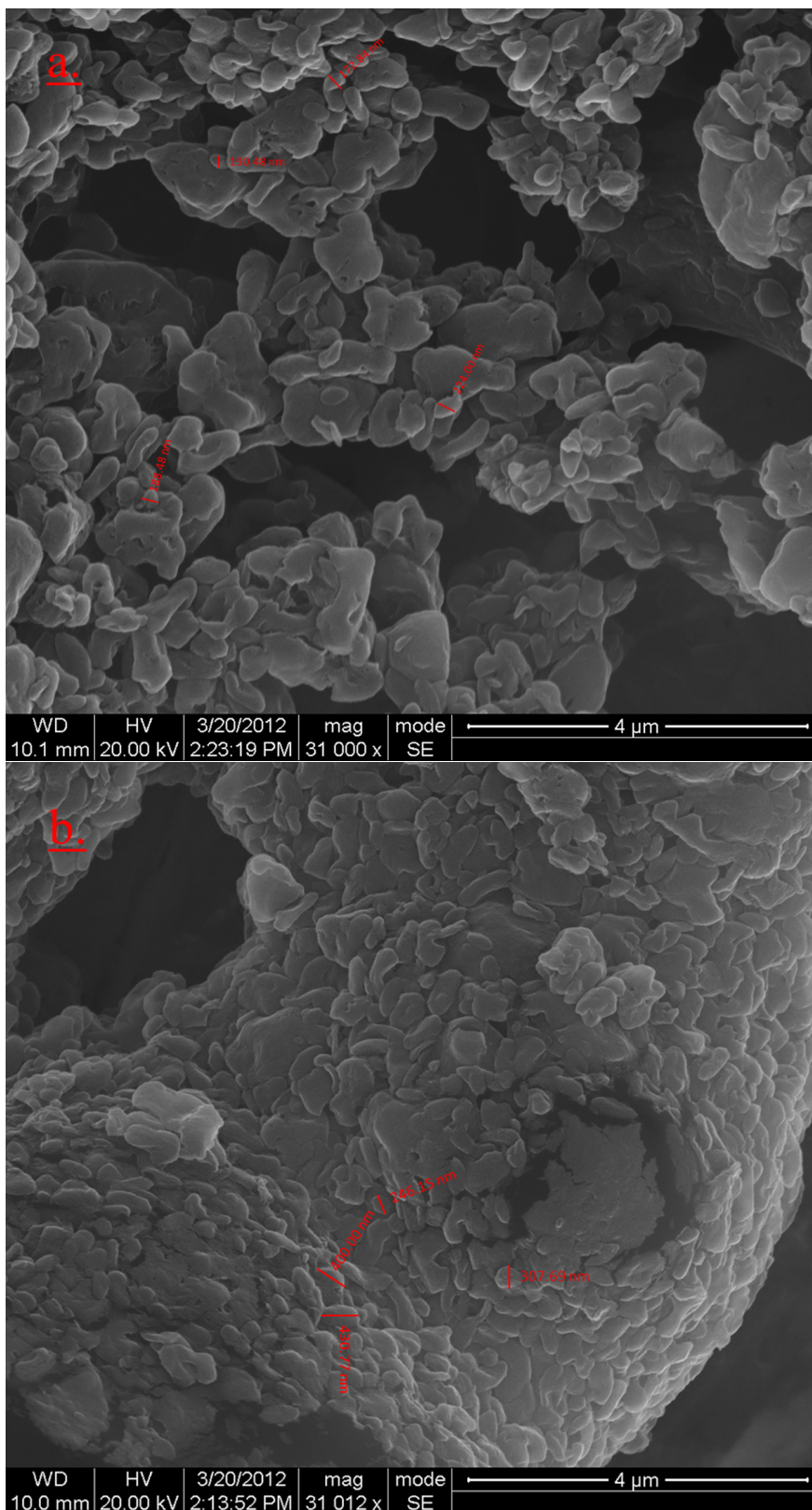


Figure. 10 - SEM images of a) PGA core nanoparticles, b) PGA/(Col/Chi)₃

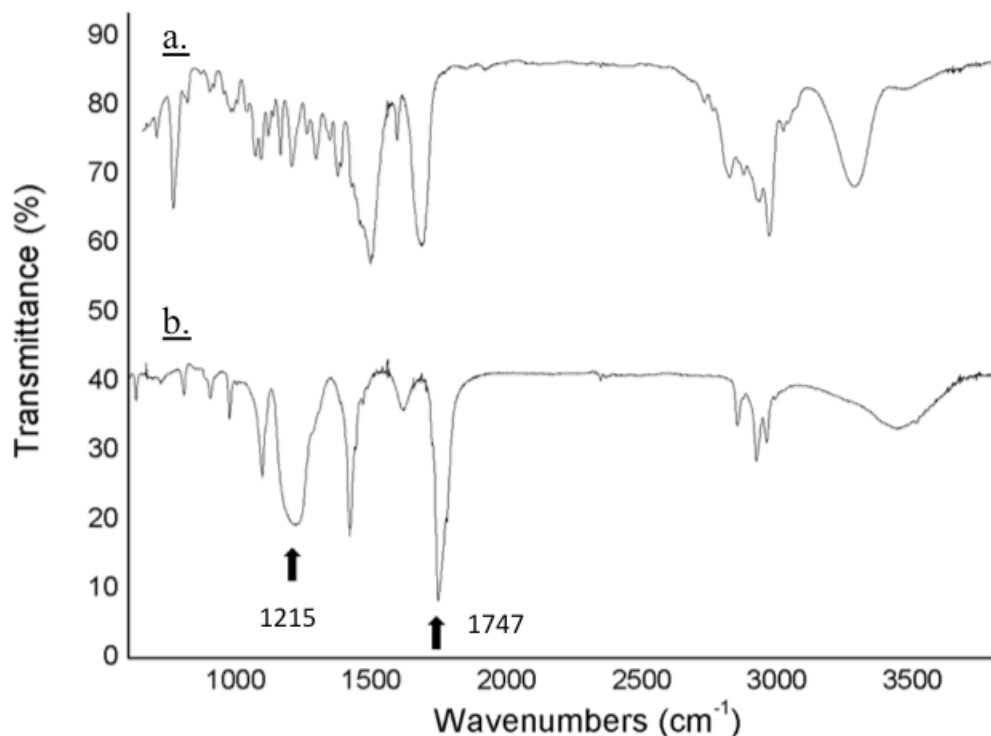


Figure. 11 – FTIR spectra for a) lidocaine, and b) lidocaine loaded PGA nanoparticles.

4.4 Zeta Potential

Fig. 12 shows the zeta potential variations along the deposition of oppositely charged type I collagen and chitosan. The PGA core particles have a positive charge of 57.47 mV. After coated with the first layer of type I collagen, the positive potential of the particles was partially neutralized to 10.73 mV. The construction of the first layer did not result in a charge overcompensation, mainly because type I collagen is weakly charged of -7.13 mV at pH ~ 8, at which the deposition was done. The subsequent adsorption of chitosan raised the charge to 49.53 mV. Although the expected charge reverse did not happen, the regular variation of charge after deposition of each new layer confirmed the layer growth.

The core nanoparticles, and the particles with one, two, and three bilayers have zeta potentials larger than 30 mV, which indicates good stability in an aqueous suspension.

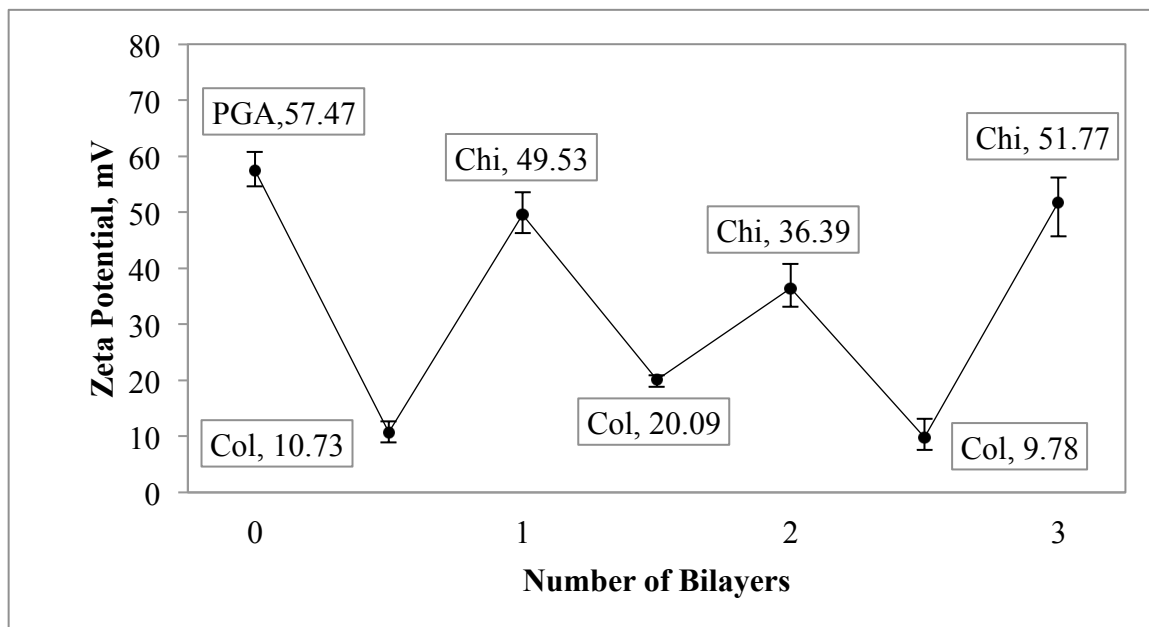


Figure. 12 – Charge variation \pm s.d. of alternative deposition of type I collagen (Col) and chitosan (Chi) on PGA nanoparticles. Data are means \pm SD; n=3.

4.5 Drug Loading

Aqueous solutions of lidocaine, type I collagen and chitosan were scanned at wavelength from 200 to 400 nm, with deionized water as a control. As shown in Fig. 13, all three substances have significant absorbance at wavelengths below 210 nm. If the wavelength is larger than 280 nm, little UV light is absorbed by each sample. At 240 nm, lidocaine showed higher absorbance compared to the other two components. Therefore, a wavelength of 240 nm was used for further quantification of lidocaine.

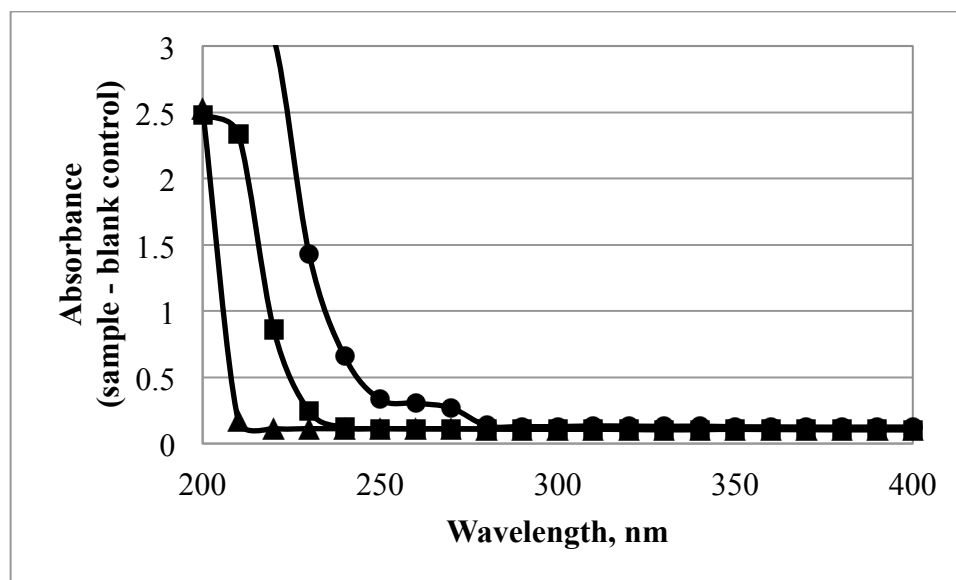


Figure. 13 - UV spectrum for 0.1 mg/ml aqueous solution of ● - lidocaine, ■ - type I collagen, and ▲ - chitosan. (Error bars were not shown because the readings were very stable; n = 3)

Since lidocaine is slightly soluble in water, standard solutions were prepared by dissolving lidocaine in deionized water to get concentrations of 0.01, 0.02, 0.03, 0.04, and 0.05 mg/ml. Each of these samples was examined at 240 nm with deionized water as control. The measured values minus the control value were plotted versus known concentrations. Fig. 14 shows a good linear correlation between the absorbance and concentration from 0.01 to 0.05 mg/ml.

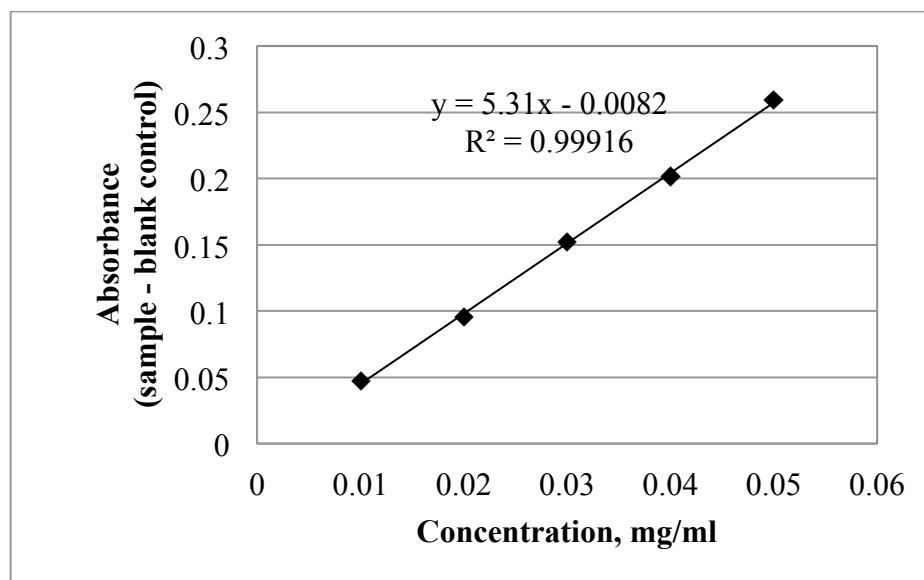


Figure. 14 – Standard curve for lidocaine from concentration of 0.01 to 0.05 mg/ml.
 (Error bars were not shown because the readings were very stable; n = 3)

The drug loading content (average and standard deviation) for four samples was calculated with Eq. (3-1), and the results are shown in Table. 3. The drug loading content decreased as the number of layers increased. The loss of drug could be due to the release into the aqueous solution during the coating process. The aqueous phases in the extraction processes were also tested. However, the concentration was too low to be detected. This result could be confirmed with the work of Wang *et al.* [80] that the solubility of lidocaine in water is only 0. 017 M, while lidocaine is freely soluble in dichloromethane.

Table. 3 – Drug loading contents for four nanoparticle samples. Data are means \pm SD;
n=3.

Sample	Drug loading content, wt. %
PGA	2.65 \pm 0.23
PGA/ Col	2.54 \pm 0.15
PGA/ (Col/Chi)	2.37 \pm 0.18
PGA/ (Col/Chi) ₃	1.82 \pm 0.20

4.6 *In vitro* Drug Release Profile

The *in vitro* drug release for the four samples was recorded and compared as shown in Fig. 15. The data in Fig. 15 Part (a) shows that for all four samples there was sustained drug release over at least 20 days, with no significant burst release. Comparing the coated particles to the uncoated particles, the release pattern shows no significant difference, although the release rates are not the same. Within the first ten hours, all the coated particles released drug at a faster rate than the uncoated particles, as shown in Fig. 15 Part (b). One possible explanation is that a small amount of lidocaine, the model drug, may have diffused to the surface of the particle during the LbL coating process. The amount of drug at or near the surface would be released first when the particles are added to an aqueous solution. Since many drugs require a double dose consisting of an initial high dose followed by a lower, sustained dose, the relatively rapid drug release from the coated nanoparticles in the first few hours is desirable for reaching the therapeutic drug level in a short period. After the first ten hours, the rate of drug release decreases and is

sustained over the 20 day test period. This indicates a near linear drug release profile for the coated nanoparticles as a trivial effect of the coated layers. Also, the release rates for particles with different number of layers are close to each other. Although the core PGA nanoparticles were coated with polymers by LbL, they were not sealed tightly and there could exist nanoscale openings among polymer fibrils. For the small molecule model drug, the openings are large enough for the drug to pass through, and the shell does not act as a barrier to the drug release. After 20 days, the release samples became nonuniform and supernatants obtained with centrifugation were not clear as those before. These changes indicate that the polymers in the core-shell nanoparticles degraded significantly, and lidocaine could not be separated from the polymer fragment by centrifugation. The broken nanoparticles could not be considered as controlled drug delivery device anymore, so the test was stopped.

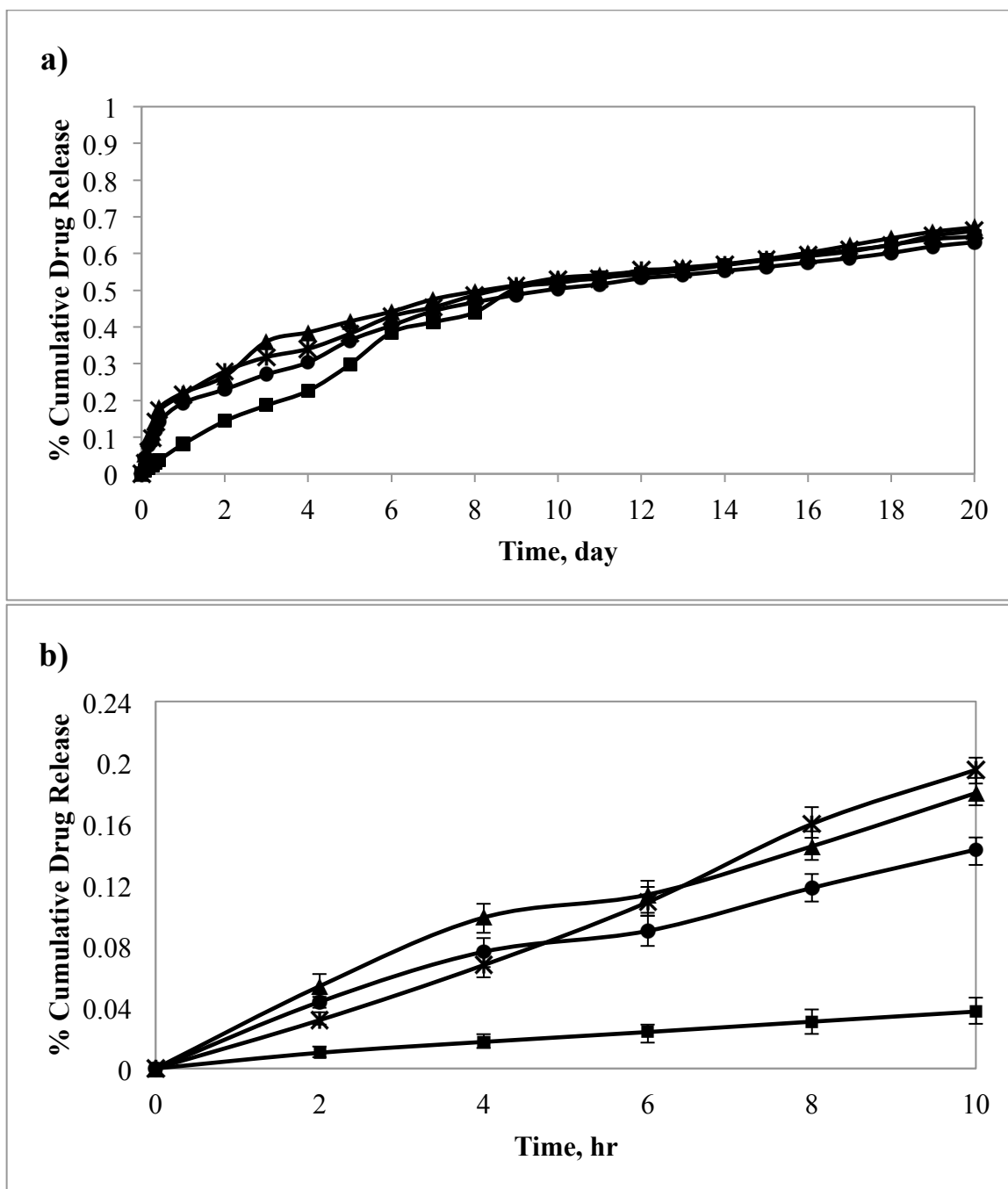


Figure. 15 - Drug release test \pm s.d. in PBS, 37.4 ° C for ■ - core nanoparticles PGA, * -PGA/(Col), ▲ -PGA/(Col/Chi), ● - PGA/(Col/Chi)₃. Error bars were not shown for Part (a), due to the small error associated with each measurement; n = 3. For Part (b), data are means \pm SD; n=3.

CHAPTER V

CONCLUSIONS AND FUTURE OUTLOOK

5.1 Conclusions

The main objective of this research was to develop a novel ocular drug delivery system to provide sustained and controlled drug release over a long period of time. The system was designed as a core-shell structured nanoparticle with the model drug entrapped within the core. PGA was selected to fabricate the core, and type I collagen and chitosan were used alternatively to construct the shell with three bilayers by LbL method, which was the most important technology used during the fabrication process.

This study demonstrated that PGA could be used to fabricate nanoparticles, and weak polyanion type I collagen and strong polycation chitosan could interact with each other through electrostatic force to form self-assembled bilayers. The resulting core-shell nanoparticles exhibited efficient drug loading content and controlled *in vitro* drug release profile sustained up to 20 days without any sudden burst.

When comparing drug loading, the content for the core nanoparticles in this study at 2.65 ± 0.23 wt. % is similar to other studies, such as reported by Braunecker et al. [55]

with theophylline loaded in PGA matrix with 5 wt. % content. Drug loading content is limited by the particle size and decreases as the size decreases. When comparing drug release, the *in vitro* drug release of the present research showed a similar zero-order pattern comparable to other nanoparticle systems, such as estrodiol (hydrophobic, Mw 272.38) loaded PLGA nanoparticles (diameter ranging from 95.4 to 583 nm) by Sahana *et al.* [81].

In comparison with other existing nonsurgical approaches, this core-shell structured nanoparticle can be expected to deliver ophthalmic drugs for weeks with several benefits. Unlike some unstable systems, the core-shell nanoparticles are stable and can be stored in a dry and cool environment for months as we use the cool stored samples to repeat experiments and see no difference. The core-shell nanoparticles can be conveniently administered in an aqueous suspension, just like the eye drops. Since an aqueous solution with low viscosity will be employed as the dispersant, the administration will not cause blurred vision as ointments do. The mucoadhesive shell of the particles can still provide a long residence time on the ocular mucous membrane, and thereby improve the bioavailability. This treatment will not involve invasive procedures as the intended use. Drug release from the core-shell nanoparticles is controlled and sustained, which reduces the reverse side effects and the administration frequency.

5.2 Future Outlook

For future studies of this novel ocular drug delivery system, the mucoadhesive properties need to be investigated, because these properties determine the residence time for the particles, which significantly affects the bioavailability. Eventually, *in vivo* testing needs to be completed for the system. *In vivo* testing provides abundant information,

including the effect of *in vivo* conditions on the drug release profile, possible irritation, degradation kinetics, and the effect on normal vision. By measuring the amount of nanoparticles administered and the *in vivo* drug release rate, the amount of total drug delivered to the tissue can be estimated. Furthermore, a mathematical model could be derived to describe the drug release from the PGA nanoparticles. Because this type of polymer degrades faster than many other polymers, such as poly(lactic-*co*-glycolic acid), the drug release will be significantly affected by both the concentration gradient as well as the polymer degradation rate, which is more complex than other systems. These additional studies will provide a better understanding of the drug release process in a quantitative manner.

REFERENCE

1. American Academy of Ophthalmology, Eye Health Statistics at a Glance, April 2011.
2. National Eye Institute, <http://www.nei.nih.gov/>.
3. Urtti, A., H. Rouhiainen, et al. (1994). "Controlled Ocular Timolol Delivery: Systemic Absorption and Intraocular Pressure Effects in Humans." Pharmaceutical Research **11**(9): 1278-1282.
4. Ogawa, Y., S. Okamoto, et al. (2001). "Successful Treatment of Dry Eye in Two Patients With Chronic Graft-versus-host Disease With Systemic Administration of FK506 and Corticosteroids." Cornea **20**(4): 430-434.
5. Urtti, A. (2006). "Challenges and obstacles of ocular pharmacokinetics and drug delivery." Advanced Drug Delivery Reviews **58**(11): 1131-1135.
6. Thrimawithana, T. R., S. Young, et al. (2011). "Drug delivery to the posterior segment of the eye." Drug Discovery Today **16**(5-6): 270-277.
7. Langer, R. (1990). "New Methods of Drug Delivery." Science **249**(4976): 1527-1533.
8. Wadhwa, S., R. Paliwal, et al. (2009). "Nanocarriers in Ocular Drug Delivery: An Update Review." Current Pharmaceutical Design **15**(23): 2724-2750.
9. Canton, I. and G. Battaglia (2012). "Endocytosis at the nanoscale." Chemical Society Reviews **41**(7): 2718-2739.
10. Zimmer, A. and J. Kreuter (1995). "Microspheres and nanoparticles used in ocular delivery systems." Advanced Drug Delivery Reviews **16**(1): 61-73.
11. Serra, L., J. Domenech, et al. (2009). "Engineering design and molecular dynamics of mucoadhesive drug delivery systems as targeting agents." European Journal of Pharmaceutics and Biopharmaceutics **71**(3, Sp. Iss. SI): 519-528.
12. Qi, H., W. Chen, et al. (2007). "Development of a poloxamer analogs/carbopol-based in situ gelling and mucoadhesive ophthalmic delivery system for puerarin." International Journal of Pharmaceutics **337**(1-2): 178-187.
13. Feng, C., Z. Xiaolin, et al. (2010). "New method for ophthalmic delivery of azithromycin by poloxamer/carbopol-based in situ gelling system." Drug Delivery **17**(7): 500-507.
14. Gratieri, T., G. M. Gelfuso, et al. (2010). "A poloxamer/chitosan in situ forming gel with prolonged retention time for ocular delivery." European Journal of Pharmaceutics & Biopharmaceutics **75**(2): 186-193.
15. Mansour, M., S. Mansour, et al. (2008). "Ocular Poloxamer-Based Ciprofloxacin Hydrochloride In Situ Forming Gels." Drug Development & Industrial Pharmacy

34(7): 744-752.

16. Wu, H., Z. Liu, et al. (2011). "Design and evaluation of baicalin-containing in situ pH-triggered gelling system for sustained ophthalmic drug delivery." International Journal of Pharmaceutics 410(1–2): 31-40.
17. Gupta, H., T. Velpandian, et al. (2010). "Ion- and pH-activated novel in-situ gel system for sustained ocular drug delivery." Journal of Drug Targeting 18(7): 499-505.
18. Pignatello, R., C. Bucolo, et al. (2002). "Flurbiprofen-loaded acrylate polymer nanosuspensions for ophthalmic application." Biomaterials 23(15): 3247-3255.
19. Pignatello, R., C. Bucolo, et al. (2002). "Eudragit RS100® nanosuspensions for the ophthalmic controlled delivery of ibuprofen." European Journal of Pharmaceutical Sciences 16(1–2): 53-61.
20. Gupta, H., M. Aqil, et al. (2010). "Sparfloxacin-loaded PLGA nanoparticles for sustained ocular drug delivery." Nanomedicine: Nanotechnology, Biology and Medicine 6(2): 324-333.
21. Lacoulonche, F., F. Gamisans, et al. (1999). "Stability and In Vitro Drug Release of Flurbiprofen-Loaded Poly-ε-Caprolactone Nanospheres." Drug Development & Industrial Pharmacy 25(9): 983.
22. Kumari, A., S. K. Yadav, et al. (2010). "Biodegradable polymeric nanoparticles based drug delivery systems." Colloids and Surfaces B: Biointerfaces 75(1): 1-18.
23. Aishwarya, S., S. Mahalakshmi, et al. (2008). "Collagen-coated polycaprolactone microparticles as a controlled drug delivery system." Journal of Microencapsulation 25(5): 298-306.
24. Park, K. (2009). "Transport across the blood-brain barrier using albumin nanoparticles." Journal of Controlled Release 137(1): 1.
25. Kang, M. K., H. Y. Lee, et al. (2010). "Release Property of Alginate Beads Coated with Poly(N-isopropylacrylamide-co-dimethylaminoethylmethacrylate)." Journal of Dispersion Science & Technology 31(12): 1685-1690.
26. Cascone, M. G., L. Lazzeri, et al. (2002). "Gelatin nanoparticles produced by a simple W/O emulsion as delivery system for methotrexate." Journal of Materials Science: Materials in Medicine 13(5): 523-526.
27. De Campos, A. M., A. Sánchez, et al. (2001). "Chitosan nanoparticles: a new vehicle for the improvement of the delivery of drugs to the ocular surface. Application to cyclosporin A." International Journal of Pharmaceutics 224(1-2): 159-168.
28. Wu, Y., W. Yang, et al. (2005). "Chitosan nanoparticles as a novel delivery system for ammonium glycyrrhizinate." International Journal of Pharmaceutics 295(1–2): 235-245.
29. Cartiera, M. S., K. M. Johnson, et al. (2009). "The uptake and intracellular fate of PLGA nanoparticles in epithelial cells." Biomaterials 30(14): 2790-2798.
30. Kakran, M., N. G. Sahoo, et al. (2010). "Fabrication of drug nanoparticles by evaporative precipitation of nanosuspension." International Journal of Pharmaceutics 383(1–2): 285-292.
31. El-Shabouri, M. H. (2002). "Positively charged nanoparticles for improving the oral bioavailability of cyclosporin-A." International Journal of Pharmaceutics 249(1–2): 101-108.

32. Janes, K. A., M. P. Fresneau, et al. (2001). "Chitosan nanoparticles as delivery systems for doxorubicin." Journal of Controlled Release 73(2–3): 255-267.
33. Jun, J. Y., H. H. Nguyen, et al. (2011). "Preparation of size-controlled bovine serum albumin (BSA) nanoparticles by a modified desolvation method." Food Chemistry 127(4): 1892-1898.
34. Gaudana, R., J. Jwala, et al. (2009). "Recent Perspectives in Ocular Drug Delivery." Pharmaceutical Research 26(5): 1197-1216.
35. Ruel-Gariépy, E. and J.-C. Leroux (2004). "In situ-forming hydrogels—review of temperature-sensitive systems." European Journal of Pharmaceutics and Biopharmaceutics 58(2): 409-426.
36. Sahoo, S. K., F. Dilnawaz, et al. (2008). "Nanotechnology in ocular drug delivery." Drug Discovery Today 13(3–4): 144-151.
37. Goldberg, M., R. Langer, et al. (2007). "Nanostructured materials for applications in drug delivery and tissue engineering." Journal of Biomaterials Science -- Polymer Edition 18(3): 241-268.
38. Vandamme, T. F. and L. Brobeck (2005). "Poly(amidoamine) dendrimers as ophthalmic vehicles for ocular delivery of pilocarpine nitrate and tropicamide." Journal of Controlled Release 102(1): 23-38.
39. Wenjun, Y., S. Kaoxiang, et al. (2010). "Preparation and characterization of puerarin–dendrimer complexes as an ocular drug delivery system." Drug Development & Industrial Pharmacy 36(9): 1027-1035.
40. Xinming, L., C. Yingde, et al. (2008). "Polymeric hydrogels for novel contact lens-based ophthalmic drug delivery systems: a review." Contact Lens & Anterior Eye: the Journal of the British Contact Lens Association 31(2): 57-64.
41. Lavik, E., M. H. Kuehn, et al. (2011). "Novel drug delivery systems for glaucoma." Eye 25(5): 578-586.
42. Koelwel, C., S. Rothschenk, et al. (2008). "Alginate Inserts Loaded with Epidermal Growth Factor for the Treatment of Keratoconjunctivitis Sicca." Pharmaceutical Development & Technology 13(3): 221-231.
43. Wang, Y., A. S. Angelatos, et al. (2008). "Template synthesis of nanostructured materials via layer-by-layer assembly." Chemistry of Materials 20(3): 848-858.
44. Zhiguo, Z., Z. Xingcai, et al. (2010). "Sonication-Assisted Synthesis of Polyelectrolyte-Coated Curcumin Nanoparticles." Langmuir 26(11): 7679-7681.
45. Zhou, J., G. Romero, et al. (2010). "Layer by layer chitosan/alginate coatings on poly(lactide-co-glycolide) nanoparticles for antifouling protection and Folic acid binding to achieve selective cell targeting." Journal of Colloid & Interface Science 345(2): 241-247.
46. Uttam, M., B. Sri, et al. (2009). "Layer-by-Layer Self-Assembly of Modified Hyaluronic Acid/Chitosan Based on Hydrogen Bonding." Biomacromolecules 10(9): 2632-2639.
- Ariga, K., Y. M. Lvov, et al. (2011). "Layer-by-layer self-assembled shells for drug delivery." Advanced Drug Delivery Reviews 63(9): 762-771.
47. Mu, B., C. Lu, et al. (2011). "Disintegration-controllable stimuli-responsive polyelectrolyte multilayer microcapsules via covalent layer-by-layer assembly." Colloids & Surfaces B: Biointerfaces 82(2): 385-390.
48. Wanunu, M., A. Vaskevich, et al. (2005). "Branched Coordination Multilayers on

- Gold." Journal of the American Chemical Society 127(50): 17877-17887.
49. Hoshi, T., S. Akase, et al. (2002). "Preparation of Multilayer Thin Films Containing Avidin through Sugar–Lectin Interactions and Their Binding Properties." Langmuir 18(18): 7024-7028.
 50. Such, G. K., A. P. R. Johnston, et al. (2011). "Engineered hydrogen-bonded polymer multilayers: from assembly to biomedical applications." Chemical Society Reviews 40(1): 19-29.
 51. Ye, S., C. Wang, et al. (2005). "Multilayer nanocapsules of polysaccharide chitosan and alginate through layer-by-layer assembly directly on PS nanoparticles for release." Journal of Biomaterials Science -- Polymer Edition 16(7): 909-923.
 52. Ariga, K., Y. M. Lvov, et al. (2011). "Layer-by-layer self-assembled shells for drug delivery." Advanced Drug Delivery Reviews 63(9): 762-771.
 53. Hurrell, S. and R. E. Cameron (2001). "Polyglycolide: Degradation and drug release. Part II: Drug release." Journal of Materials Science: Materials in Medicine 12(9): 817-820.
 54. Hurrell, S. and R. E. Cameron (2001). "Polyglycolide: degradation and drug release. Part I: Changes in morphology during degradation." Journal of Materials Science: Materials in Medicine 12(9): 811-816.
 55. Braunecker, J., M. Baba, et al. (2004). "The effects of molecular weight and porosity on the degradation and drug release from polyglycolide." International Journal of Pharmaceutics 282(1-2): 19-34.
 56. Duvvuri, S., S. Majumdar, et al. (2003). "Drug delivery to the retina: challenges and opportunities." Expert Opinion on Biological Therapy 3(1): 45-56.
 57. Ali, Y. and K. Lehmussaari (2006). "Industrial perspective in ocular drug delivery." Advanced Drug Delivery Reviews 58(11): 1258-1268.
 58. Choonara, Y. E., V. Pillay, et al. (2010). "A Review of Implantable Intravitreal Drug Delivery Technologies for the Treatment of Posterior Segment Eye Diseases." Journal Of Pharmaceutical Sciences 99(5): 2219-2239.
 59. Fathima, N. N., M. C. Bose, et al. (2006). "Stabilization of type I collagen against collagenases (type I) and thermal degradation using iron complex." Journal of Inorganic Biochemistry 100(11): 1774-1780.
 60. Rudakova, T. E. and G. E. Zaikov (1987). "Degradation of collagen and its possible applications in medicine." Polymer Degradation and Stability 18(4): 271-291.
 61. Miao, X., Y. Liu, et al. (2010). "Layer-by-layer assembly of collagen and electroactive myoglobin." Bioelectrochemistry 79(2): 187-192.
 62. Zhang, J., B. Senger, et al. (2005). "Natural polyelectrolyte films based on layer-by layer deposition of collagen and hyaluronic acid." Biomaterials 26(16): 3353-3361.
 63. Sung Mook, L., S. Dae Kun, et al. (2008). "In vitro and in vivo degradation behavior of acetylated chitosan porous beads." Journal of Biomaterials Science -- Polymer Edition 19(4): 453-466.
 64. Ludwig, A. (2005). "The use of mucoadhesive polymers in ocular drug delivery." Advanced Drug Delivery Reviews 57(11): 1595-1639.

65. de Villiers, M. M. and Y. M. Lvov (2011). "Layer-by-layer self-assembled nanoshells for drug delivery." Advanced Drug Delivery Reviews 63(9): 699-700.
66. Nagarwal, R. C., S. Kant, et al. (2009). "Polymeric nanoparticulate system: A potential approach for ocular drug delivery." Journal of Controlled Release 136(1): 2-13.
67. Gorle, A. P. and S. G. Gattani (2010). "Development and evaluation of ocular drug delivery system." Pharmaceutical Development & Technology 15(1): 46-52.
68. Lang, J. C. (1995). "Ocular drug delivery conventional ocular formulations." Advanced Drug Delivery Reviews 16(1): 39-43.
69. Sharma, M. (2010). "Development of a novel nanotechnology-based ophthalmic drug delivery device." (Master's thesis) Oklahoma State University. <http://search.proquest.com/docview/755491980?accountid=4117>.
70. Geroski, D. H. and H. F. Edelhauser (2000). "Drug Delivery for Posterior Segment Eye Disease." Investigative Ophthalmology & Visual Science 41(5): 961-964.
71. Xie, Y.-L., M.-J. Wang, et al. (2009). "Preparation and Characterization of Biocompatible Microcapsules of Sodium Cellulose Sulfate/Chitosan by Means of Layer-by-Layer Self-Assembly." Langmuir 25(16): 8999-9005.
72. Manju, S. and K. Sreenivasan (2011). "Hollow microcapsules built by layer by layer assembly for the encapsulation and sustained release of curcumin." Colloids & Surfaces B: Biointerfaces 82(2): 588-593.
73. Yong-Hua, J., L. Yan, et al. (2010). "Layer-by-Layer Assembly of Poly(lactic acid) Nanoparticles: A Facile Way to Fabricate Films for Model Drug Delivery." Langmuir 26(11): 8270-8273.
74. Yan, S., J. Zhu, et al. (2011). "Layer-by-layer assembly of poly(l-glutamic acid)/chitosan microcapsules for high loading and sustained release of 5-fluorouracil." European Journal of Pharmaceutics and Biopharmaceutics 78(3): 336-345.
75. Grech, J. M. R., J. F. Mano, et al. (2008). "Chitosan Beads as Templates for Layer-by-Layer Assembly and their Application in the Sustained Release of Bioactive Agents." Journal of Bioactive & Compatible Polymers 23(4): 367-380.
76. Chujo, K., H. Kobayashi, et al. (1967). "Physical and chemical characteristics polyglycolide." Die Makromolekulare Chemie 100(1): 267-270.
77. Luescher, M., M. Rüegg, et al. (1974). "Effect of hydration upon the thermal stability of tropocollagen and its dependence on the presence of neutral salts." Biopolymers 13(12): 2489-2503.
78. Li, Y., M. Hu, et al. (2010). "Controlling the functional performance of emulsion-based delivery systems using multi-component biopolymer coatings." European Journal of Pharmaceutics & Biopharmaceutics 76(1): 38-47.
79. Wikipedia, <http://en.wikipedia.org/>.
80. Wang, J., T. Hou, et al. (2009). "Aqueous Solubility Prediction Based on Weighted Atom Type Counts and Solvent Accessible Surface Areas." Journal of Chemical Information and Modeling 49(3): 571-581.
81. Sahana, D. K., G. Mittal, et al. (2008). "PLGA nanoparticles for oral delivery of hydrophobic drugs: Influence of organic solvent on nanoparticle formation and release Behavior in vitro and in vivo using estradiol as a model drug." Journal Of

- Pharmaceutical Sciences **97**(4): 1530-1542.
82. Lai, S. K., Y.-Y. Wang, et al. (2009). "Mucus-penetrating nanoparticles for drug and gene delivery to mucosal tissues." Advanced Drug Delivery Reviews 61(2): 158-171.
 83. Patravale, V. B., A. A. Date, et al. (2004). "Nanosuspensions: a promising drug delivery strategy." Journal of Pharmacy and Pharmacology 56(7): 827-840.
 84. Yan, Y., G. K. Such, et al. (2011). "Toward Therapeutic Delivery with Layer-by-Layer Engineered Particles." ACS Nano 5(6): 4252-4257.
 85. Hurrell, S. and R. E. Cameron (2003). "The effect of buffer concentration, pH and buffer ions on the degradation and drug release from polyglycolide." Polymer International 52(3): 358-366.

VITA

Meng Wang

Candidate for the Degree of

Master of Science

Thesis: APPLICATION OF LAYER-BY-LAYER ASSEMBLY FOR CONTROLLED
DRUG RELEASE FROM POLYGLYCOLIDE NANOPARTICLES

Major Field: Chemical Engineering

Biographical:

Education:

Completed the requirements for the Master of Science in Chemical Engineering at Oklahoma State University, Stillwater, Oklahoma in December, 2012.

Completed the requirements for the Bachelor of Engineering in Pharmaceutical Engineering at Tianjin University, Tianjin, China in July, 2009.

Experience:

- Designed a novel core-shell structured nanoparticle for controlled ophthalmic drug delivery
- Conducted synthesis and characterization of the designed device
- Lab management including purchase of supplies, equipment maintenance, and waste disposal
- Other projects in process simulation and process control

Professional Memberships:

OSU Automation Society

Name: Meng Wang

Date of Degree: December, 2012

Institution: Oklahoma State University

Location: Stillwater, Oklahoma

Title of Study: APPLICATION OF LAYER-BY-LAYER ASSEMBLY FOR
CONTROLLED DRUG RELEASE FROM POLYGLYCOLIDE NANOPARTICLES

Pages in Study: 58

Candidate for the Degree of Master of Science

Major Field: Chemical Engineering

Over the past years, topical ophthalmic drug administration has been limited due to low bioavailability. Conventional eye drops have approximate 95% loss, and the washout can result in significant side effects. Ointment was employed to prolong the residence time of the drug at the eye surface, but the application can result in irritation and blurry vision. Although some invasive methods (ex. intravitreal injection) were developed for direct delivery of the drug, these methods have various drawbacks, such as poor patient compliance and possibility of retina detachment by frequent applications.

To improve sustained delivery of drugs to the eye in a non-invasive way, we designed a novel core-shell nanoparticle that can be easily applied in a suspension. The core nanoparticles were fabricated by loading lidocaine as a model drug within polyglycolide nanoparticles. Then the core nanoparticles were coated alternatively with oppositely charged type I collagen and chitosan to obtain multilayers.

FTIR spectra and variation of zeta potential were employed to demonstrate successful drug loading in the core and layer growth of the shell, respectively. The resulting core-shell nanoparticles were found to be oval in shape, 391.2 ± 4.5 nm in diameter, and loaded with 1.82 ± 0.20 wt. % of lidocaine (model drug). The in vitro drug release was measured for 20 days showing no sudden burst and close to a first order release profile. The shell showed slight modification of release rate at the beginning of the release test.

ADVISER'S APPROVAL: Dr. Heather Fahlenkamp
